
Wally Pacholka

VNIVERSITAT DE VALÈNCIA

Cosmic Architecture: Numerical Simulations in Astrophysics and Cosmology

José-María Ibáñez

Departamento de Astronomía y Astrofísica
Universidad de Valencia, España

Scientific Meeting of the Spanish Astronomical Society

Valencia, July 9-13, 2012

Scheme

Outline

Supercomputing: Some headlines

Numerical simulation

has emerged as the third methodology alongside observation/experimentation and analytic theory. It is (together with theory and observation/experimentation) one of the three basic paradigmes for the advancing of science and engineering (M. Norman)

Grand Challenge applications

Computation-intensive fundamental problems in science and engineering whose solutions can only be advanced by applying high performance computing (HPC) and communications technologies and resources.

Supercomputing

- *To computationally solve Grand Challenge applications that will enable us to learn, understand, model, use and/or predict complex dynamic systems.*
- It has become an **essential tool for scientific and technological progress in the areas of science and engineering.** A common feature of these Grand Challenges is that they involve simulation. In order to be able to generate results equivalent to the ones obtained by physical experimentation, these simulations require an extremely high number of operations and manipulate extremely huge volumes of data.

Supercomputing in Astrophysics and Cosmology

Numerical simulations in Astrophysics and Cosmology

To elucidate complex dynamical behavior contained within a theoretical model, and/or to reproduce an observation, and/or to guide astronomers toward new observational strategies, and/or to predict new phenomena $\Longrightarrow$ **Supercomputers.**

Some estimates

Let us assume a typical numerical problem of solving a system of PDEs (e.g, fluid dynamics) with standard difference schemes $\Longrightarrow$ *number of points, n,* to solve a given *spatial scale, L,* into a spatial domain spanning *X times* the spatial scale L $\Longrightarrow$ In 3D (three spatial dimensions): $(X * n)^3 \Longrightarrow P = (100 * 10)^3 = 10^6$ **points**
Let us consider a computer having a *clock frequency* f *GHz*, and executing an arithmetic operation each z *CPU cycles*. $\mathcal{O}$ **is the number of arithmetic operations at each point.** $\Longrightarrow$ **Total time:** $T = P * \left(\mathcal{O} * \left(\frac{\mathrm{z}}{\mathrm{f}}\right)\right)$

Typical values: $f = 2$ **GHz,** $z = 4$, $\mathcal{O} = 1.000$, $P = 10^6 \Longrightarrow T = 2000$ **s** ≈ 33 **min.**

Evolution problem *(number of timesteps* ≈ 15000*)* $\Longrightarrow$ $T \approx 1$ **year,**

$\Longrightarrow$ **To solve the problem using parallel programming in multiprocessors supercomputers.**

Milestones in Scientific Computing (Ia) *Adapted from J. Ruttimann, Nature, vol 440 (2006)*

Year	Invention	Inventor
3000 BC	Abacus	Chinese
1642	Pascaline : Mechanical adding machine	Blaise Pascal
1843	Computer program	Ada Lovelace
1890	Punch card machine	Herman Hollerith
1940	Turing machine	Alan M. Turing **(1912-1954)**
1944	Mark I	Howard Aiken
1946	ENIAC (Electronic Numerical Integrator and Calculator)	J.W. Mauchley & J. Presper Eckert
1947	Transistor:semiconductor device alternative to the vacuum tube	J.Bardeen, W.Brattain & W. Shockley
1951	Random Access Memory	Jay Forrester
1952	Computer compiler	Grace Hopper
1958	Integrated circuit (also known as: IC, microcircuit, microchip, silicon chip, or chip)	Jack Kilby
1958	Video Game	William Higinbotham
1966	Hand-held calculator	J.Kilby, J.D. Merryman & J.H. Van Tassel
1967	ARPANET (the predecessor of the Internet)	US Dept. of Defense
1967	LSI (large-scale integration) technology yielded two devices: RAM-chip & microprocessor	
1967	Dynamic Random Access Memory	Robert Dennard
1968	Microprocessor (" a computer on a chip") IC that contains all the arithmetic, logic, and control circuitry necessary to serve as a central processing unit (CPU)	Ted Hoff

Milestones in Scientific Computing (Ib) *Adapted from J. Ruttimann, Nature, vol 440 (2006)*

Year	Invention	Inventor
1969	First coupled ocean-atmosphere general circulation model	S. Manabe & K. Bryan
1971	First computerized tomography scanner	
1971	Protein Data Bank	Brookhaven NL, NY
1972	HP-35: first hand-held scientific calculator	Hewlett-Packard
1973	Internet	Vinton Cerf
1976	First CRAY supercomputer	S. Cray, Los Alamos
1976	Personal Computer	S. Jobs & S. Wozniak
1977	PC modem	D. Hayes & D. Heatherington
1983	Connection Machine:the first supercomputer to feature parallel processing	Danny Hillis
1989	World Wide Web	Tim Berners-Lee, CERN
1996	Shotgun technique uses computers to piece together large fragments of DNA code $\Longrightarrow$ sequencing of the entire human genome	Craig Venter
2001	The National Virtual Observatory:to develop methods for mining huge astronomical data sets	USA
2001	BIRN(Biomedical Informatics Research Network) a grid of supercomputers designed to let multiple institutions share data	USA
2005	Blue Gene family of supercomputers	IBM, USA
2012	Sequoia Blue Gene family (1.5 Mcores)	IBM, USA

TOP500® JUNE 2012

PRESENTED BY UNIVERSITY OF MANNHEIM

ICL UT INNOVATIVE COMPUTING LABORATORY THE UNIVERSITY of TENNESSEE

BERKELEY LAB Lawrence Berkeley National Laboratory

FIND OUT MORE AT www.top500.org

	NAME	SPECS	SITE	COUNTRY	CORES	R_{max} Pflop/s
1	**Sequoia**	IBM BlueGene/Q, Power BQC 16C 1.60 GHz, Custom interconnect	DOE / NNSA / LLNL	USA	1,572,864	16.33
2	**K computer**	Fujitsu SPARC64 VIIIfx 2.0GHz, Tofu interconnect	RIKEN AICS	Japan	705,024	10.51
3	**Mira**	IBM BlueGene/Q, Power BQC 16C 1.60 GHz, Custom interconnect	DOE / SC / ANL	USA	786,432	8.153
4	**SuperMUC**	IBM iDataPlex DX360M4, Xeon E5-2680 8C 2.70GHz, Infiniband QDR	Leibniz Rechenzentrum	Germany	147,456	2.897
5	**Tianhe-1A**	NUDT YH MPP, Xeon X5670 6C 2.93 GHz, NVIDIA 2050	NUDT/NSCC/Tianjin	China	186,368	2.566

PERFORMANCE DEVELOPMENT

PROJECTED

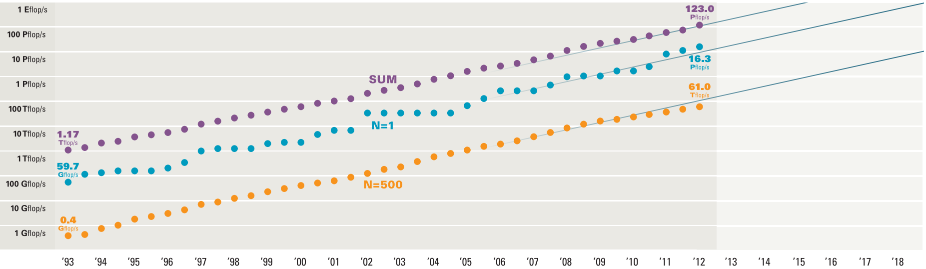

Leibniz-Rechenzentrum (LRZ): SuperMUC Petascale System @ Garching bei München

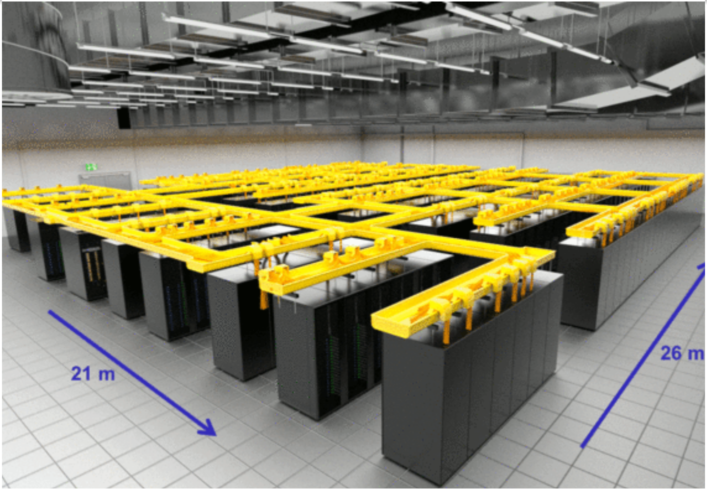

- 155,656 processor cores in 9400 compute nodes.
- Peak performance of 3 Petaflop/s.
- SuperMUC is integrated into the European High Performance Computing ecosystem.

http://www.lrz.de/services/compute/supermuc/systemdescription/
LRZ will act as an *European Centre for Supercomputing* and will be Tier-0 centre of PRACE.

Milestones in Scientific Computing (IIa): *Spain in the 70's*

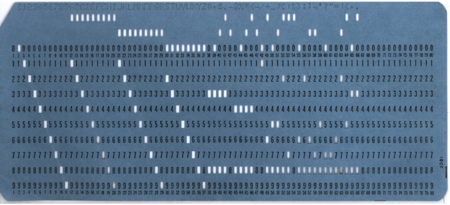

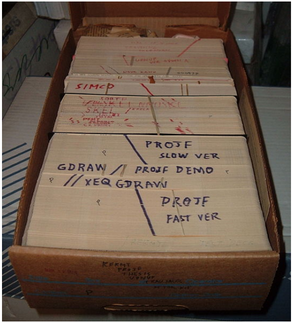

Punched cards

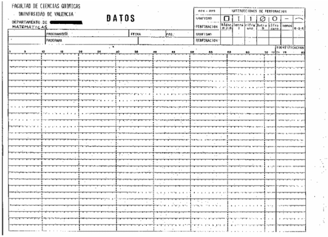

Programming sheet

Milestones in Scientific Computing (IIb): *Mare-Nostrum (2005) @ the BSC-CNS*

Milestones in Scientific Computing (IIc): *BSC-CNS & RES*

Red Española de Supercomputación

MareNostrum

Proceso:	10240 PowerPC 970 2.3 GHz
Memoria:	20 TBytes
Disco:	280 + 90 TBytes
Redes:	Myrinet, Gigabit, 10/100
Sistema:	Linux

CeSViMa

Proceso:	2408 PowerPC 970 2.2 GHz
Memoria:	4.7 TBytes
Disco:	63 + 47 TBytes
Redes:	Myrinet, Gigabit, 10/100
Sistema:	Linux

IAC, UMA, UNICAN, UNIZAR, UV

Proceso:	512 PowerPC 970 2.2 GHz
Memoria:	1 TByte
Disco:	14 + 10 TBytes
Redes:	Myrinet, Gigabit, 10/100
Sistema:	Linux

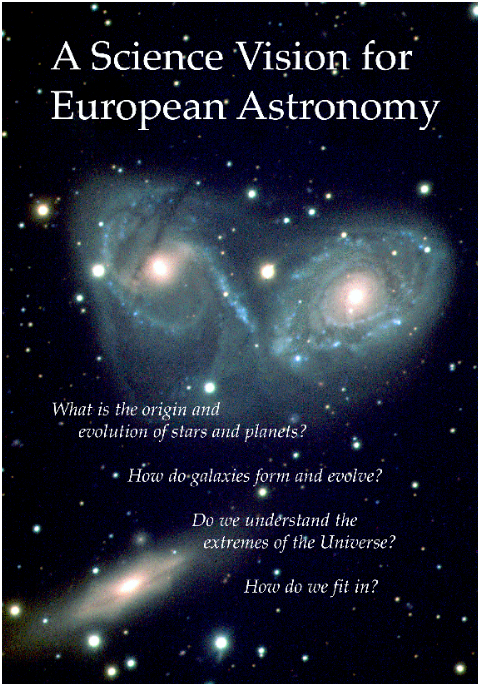

ASTRONET, *A Science Vision for European Astronomy* *(January, 2007)*
http://www.astronet-eu.org/Science-questions

Funding agencies from a number of European countries established ASTRONET, an ERA-net with financial support from the EU, to develop a comprehensive strategic plan for European astronomy covering the ambitions of all of astronomy, ground and space, including links with neighbouring fields, to establish the most effective approach towards answering the highest priority scientific questions.

ASTRONET, A Science Vision for European Astronomy: *Science questions*

Panel A : *Do we understand the extremes of the Universe?*

- How did the Universe begin?
- What is dark matter and dark energy?
- Can we observe strong gravity in action?
- How do supernovae and gamma-ray bursts work?
- How do black hole accretion, jets and outflows operate?
- What do we learn about the Universe from energetic radiation and particles?

Panel B : *How do galaxies form and evolve?*

- How did the universe emerge from its dark ages?
- How did the structure of the cosmic web evolve?
- Where are most of the chemical elements throughout cosmic time?
- What is the cycling of stars, gas and dust in galaxies?
- How did the Milky Way form?

Panel C : *What is the origin and evolution of stars and planetary systems?*

- How do stars and stellar systems form?
- Is the initial mass function of stars universal?
- What do we learn by probing stellar interiors?
- What is the life-cycle of the ISM and stars?
- How do planetary systems form and evolve?
- What are the demographics of planets in the Galaxy? How do we tell which planets harbour life?

Panel D : *How do we fit in?*

- How do we study the Sun to explore fundamental astrophysical processes?
- What drives Solar variability on all scales?
- What is the impact of Solar Variability on life on Earth?
- What is the dynamical history of the Solar system?
- What can we learn from Solar system exploration about its formation and evolution?
- Where should we look for life in the Solar system?

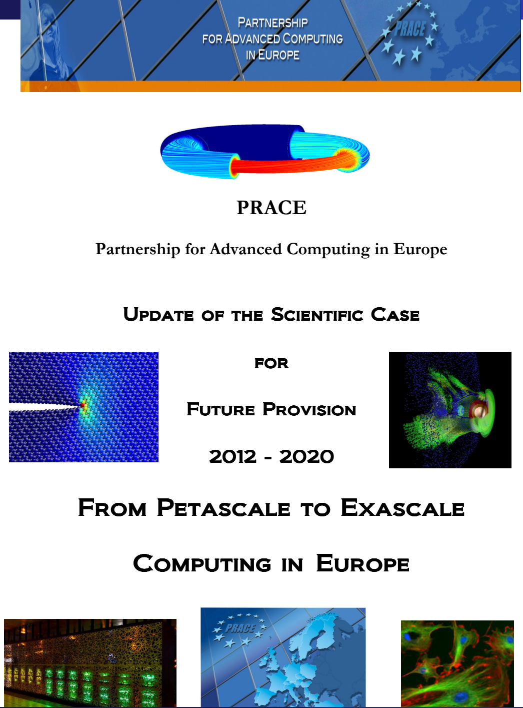

PARTNERSHIP FOR ADVANCED COMPUTING IN EUROPE

PRACE

PRACE

Partnership for Advanced Computing in Europe

UPDATE OF THE SCIENTIFIC CASE

FOR

FUTURE PROVISION

2012 - 2020

FROM PETASCALE TO EXASCALE

COMPUTING IN EUROPE

PRACE

Grand Challenges

1. What is the identity of the cosmic dark matter and dark energy?
2. How did the universe emerge from the dark ages immediately following the Big Bang?
3. **How did galaxies form?**
4. **How do galaxies and quasars evolve chemically and dynamically and what is the cause of their diverse phenomenology?**
5. How does the chemical enrichment of the universe take place?
6. How do stars form?
7. **How do stars die?**
8. How do planets form?
9. Where is life outside the Earth?
10. **How magnetic fields in the universe are generated and what role do they play in particle acceleration and other plasma processes?**
11. **How can we unravel the secrets of the sources of strongest gravity?**
12. **What will as yet unexplored windows into the universe such as neutrinos and gravitational waves reveal?**

Outline

Euler Equations for Ideal Fluids as a Hyperbolic System of Conservation Laws (HSCL)

Euler Equations $\Rightarrow$ HSCL

$$\frac{\partial \mathbf{u}}{\partial t} + \frac{\partial \mathbf{f}^i(\mathbf{u})}{\partial x^i} = \mathbf{s}(\mathbf{u})$$

$$\begin{aligned}
\mathbf{u} &= \left(\rho,\ \rho v^j,\ e\right) \\
\mathbf{f}^i(\mathbf{u}) &= \left(\rho v^i,\ \rho v^i v^j + p\delta^{ij},\ (e+p)v^i\right) \\
\mathbf{s}(\mathbf{u}) &= \left(0,\ -\rho\frac{\partial \Phi}{\partial x^j} + Q^j_M,\ -\rho v^i \frac{\partial \Phi}{\partial x^i} + Q_E + v^i Q^i_M\right)
\end{aligned}$$

$\mathbf{u}$ is the **vector of conserved variables**.
$\mathbf{f}^i(\mathbf{u})$ are the **fluxes** in each spatial direction i.
$\mathbf{s}(\mathbf{u})$ are the **sources**.
Q^i_M, Q_E are, for example, the sources coming from the coupling matter-radiation.
Φ is the *Newtonian gravitational potential*, which obeys *Poisson's equation*: $\Delta\Phi = 4\pi G\rho$
An *equation of state* $p = p(\rho, \epsilon)$ closes the system.

Radiation-magnetohydrodynamic equations , *Henney, Arthur, De Colle & Mellema (2009)*

$$\frac{\partial \rho}{\partial t} + \nabla \cdot (\rho \vec{v}) = 0$$

$$\frac{\partial \rho \vec{v}}{\partial t} + \nabla \cdot \left(\rho \vec{v}\vec{v} + p_{\rm tot} I - \vec{B}\vec{B} \right) = 0$$

$$\frac{\partial e}{\partial t} + \nabla \cdot \left((e + p_{\rm tot})\, \vec{v} - (\vec{v} \cdot \vec{B}\,)\vec{B} \right) = H - L$$

$$\frac{\partial \vec{B}}{\partial t} + \nabla \cdot \left(\vec{v}\vec{B} - \vec{B}\vec{v} \right) = 0$$

L and H are, respectively, the microphysical cooling and heating rates.

Coupling of MHD with chemical reactions and the ionising radiation field

$$\frac{\partial\, n_{\rm n}}{\partial t} + \nabla \cdot (n_{\rm n} \vec{v}) = n_{\rm p}\, n_{\rm e}\, \alpha(T) - n_{\rm n} \left(n_{\rm e} C(T) + \int_{\nu_0}^{\infty} \sigma_\nu (4\pi J_\nu / h\nu)\, d\nu \right),$$

$n_{\rm p}$, $n_{\rm n}$, $n_{\rm e}$ $\Longrightarrow$ number densities of ionised and neutral hydrogen, and electrons.
$\alpha(T)$, $C(T)$ $\Longrightarrow$ radiative recombination and collisional ionisation coefficients.
σ_ν, J_ν $\Longrightarrow$ photoionization cross-section and local mean intensity:

$$4\pi J^*_\nu(\vec{r}) = \frac{\mathcal{L}^*_\nu\, e^{-\tau_\nu}}{4\pi |\vec{r} - \vec{r}_*|^2} \quad , \quad \tau_\nu = \int_0^{|\vec{r}-\vec{r}_*|} n_{\rm n}\, (\vec{r}_* + s\, \vec{e}_r)\, \sigma_\nu\, ds$$

Pillars of creation: Star EGGs in the Eagle Nebula *(Credit: Hester & Scowen, HST, NASA)*

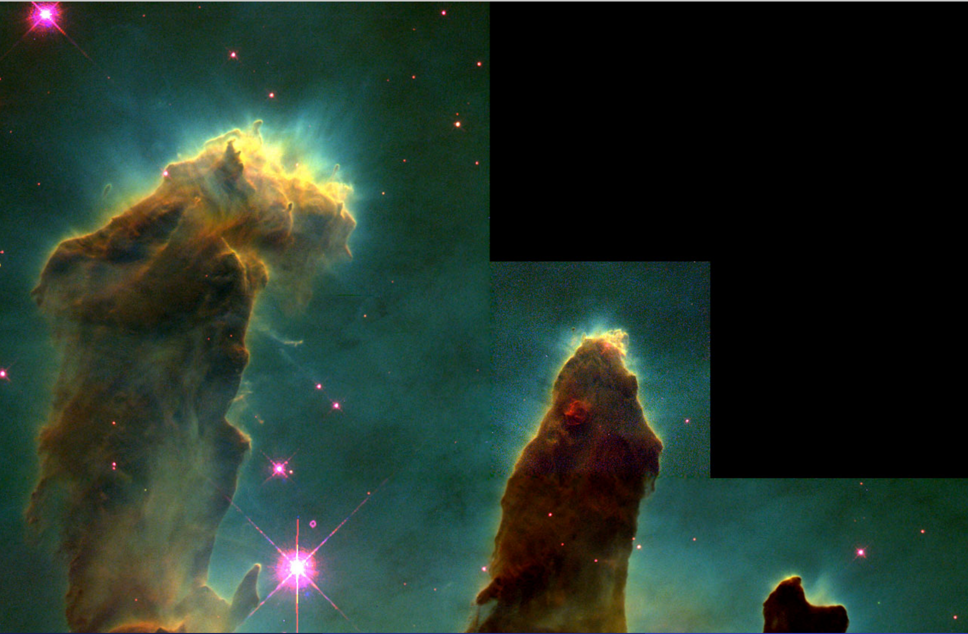

A photoevaporating magnetic globule (sketch) , *Henney, Arthur, De Colle & Mellema (2009)*

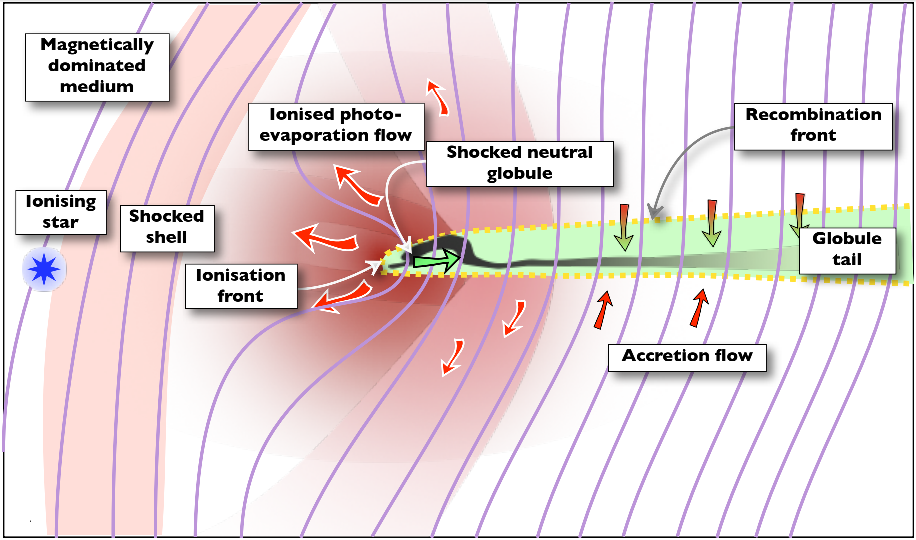

Ionised gas (red), neutral/molecular gas (green), and magnetic field lines (purple). The orientation of an initial magnetic field is:$\theta_0 \sim 80°$.

Radiation-MHD simulations: Photoionisation of magnetised globules , *Henney et al, 2009*

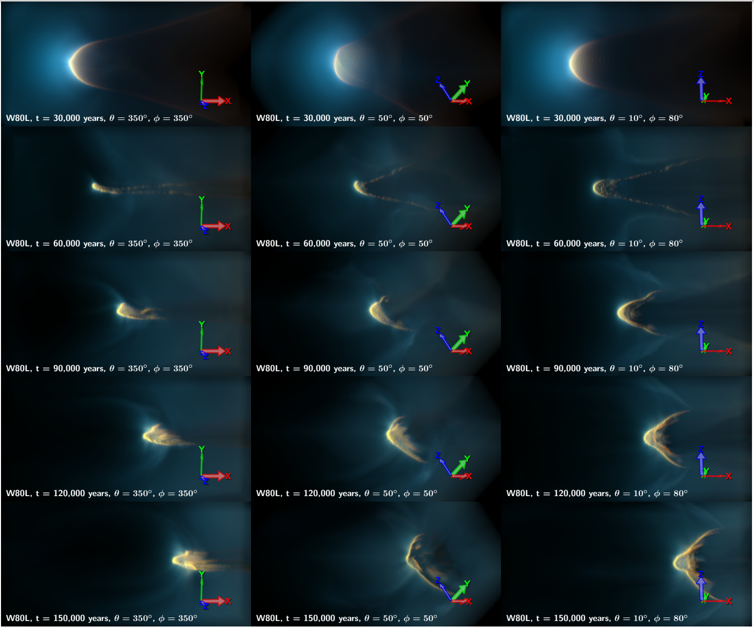

Sideways view of the ionised emission for a sequence of evolutionary times from 30,000 to 150,000 years (top to bottom). The colours represent the surface brightness in three optical emission lines: $[N\ II]\ 6584\ \mathring{A}$ (red), $H_\alpha\ 6563\ \mathring{A}$ (green), and $[O\ III]\ 5007\ \mathring{A}$ (blue). Yellow-orange colours trace the ionisation front on the surface of the globule, while blue-green trace highly ionised gas. Left column shows the view from the side, slightly in front and slightly above. Central column shows the view from behind and below. Right column shows the view from below.

A Complete Solar Cycle from SOHO *(Credit: SOHO - EIT Consortium, ESA, NASA, 2007)*

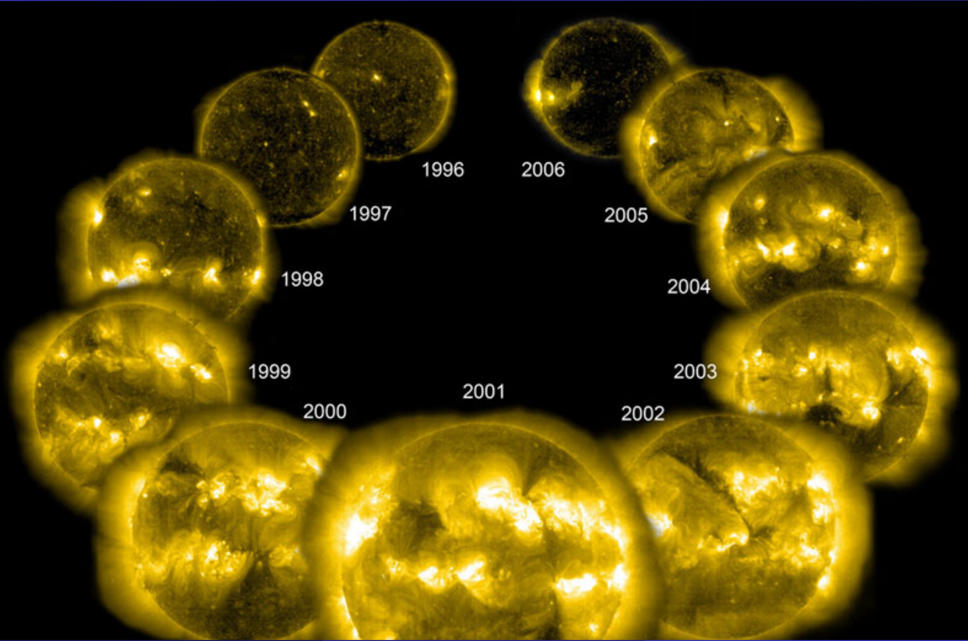

Granules and Bright Points on the Quiet Sun *(Credit: J. Sánchez-Almeida et al., IAC, 2010)*

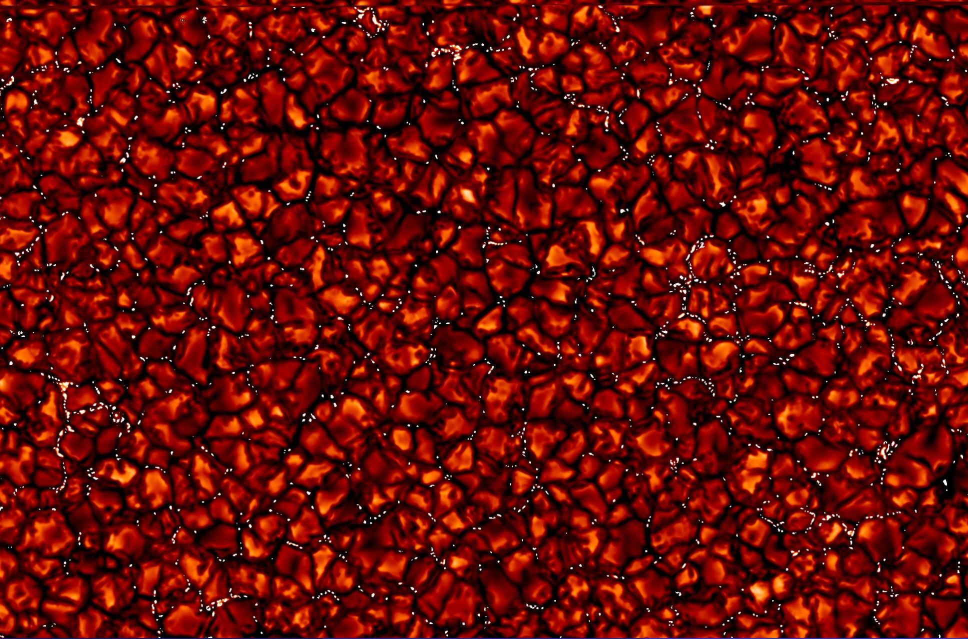

Our active Sun: A Jet from the Sun *(Credit: Hinode, JAXA, NASA)*

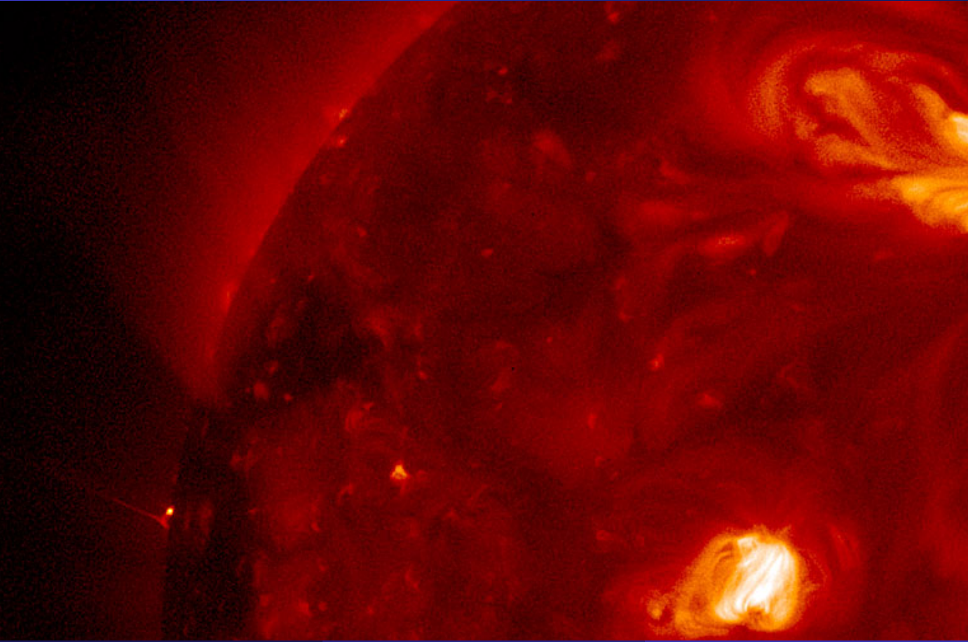

Solar Abundance Corrections derived through 3D-Magnetoconvection Simulations

Fabbian, Khomenko, Moreno-Insertis & Nordlund (2010)

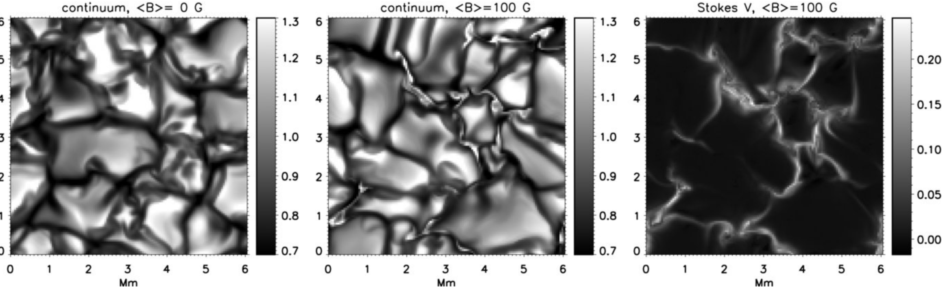

Emerging continuum intensity at 608 nm in the HD simulation run (left) and in the MHD run with "100 G" setup (center). Note the appearance of intergranular bright points after introducing magnetic flux. The right panel shows the amplitude of Stokes V, defined as $max \mid V \mid$ *in units of the continuum intensity, sign included.*

Jets in Coronal Holes: Hinode Observations and Three-dimensional Computer Modeling

Moreno-Insertis, Galsgaard, & Ugarte-Urra (2008)

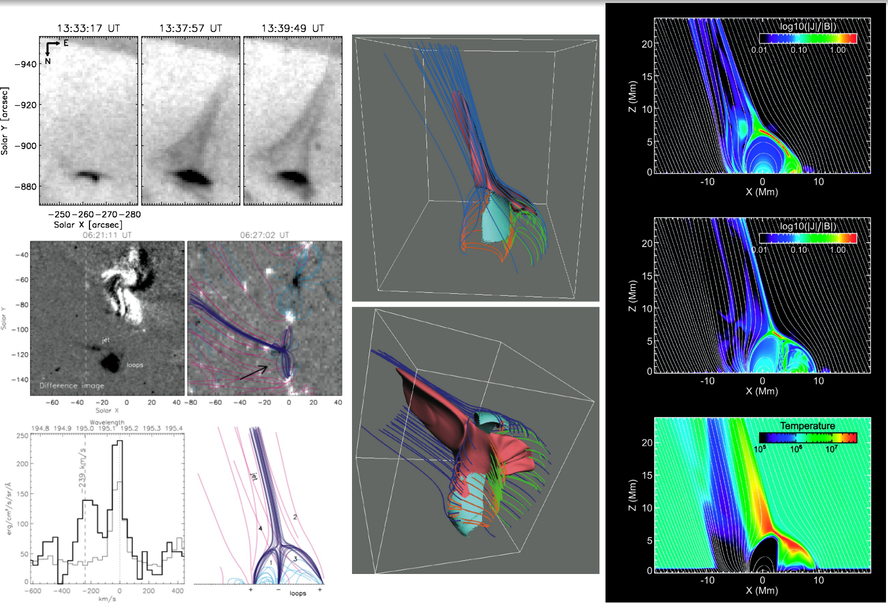

Astrophysical scenarios governed by (magneto-)hydrodynamical processes:

Planetary Nebulae *Interacting stellar winds, cooling and heating, gravity, ...* *(Credits: Balick et al. & NASA)*

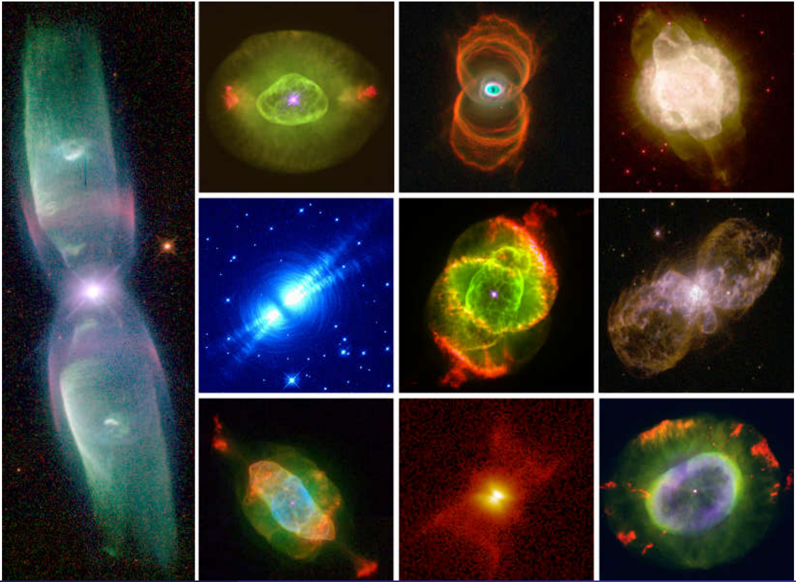

From Bipolar to Elliptical: Simulating the Morphological Evolution of Planetary Nebulae

Huarte-Espinosa, Frank, Balick, Blackman, De Marco, Kastner & Sahai (2011)

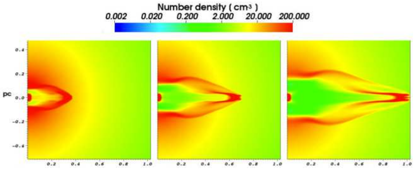

Model 1: spherical AGB wind → jet. Time={4059, 8644, 13283} yr, from left to right.

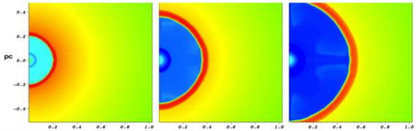

Model 2: spherical AGB wind → fast wind. Time={4342, 8676, 13006} yr, from left to right.

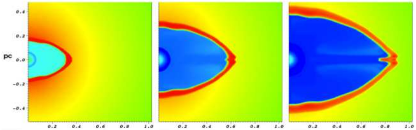

Model 3: spherical AGB wind → jet → fast wind. Time={3605, 7200, 10791} yr, from left to right.

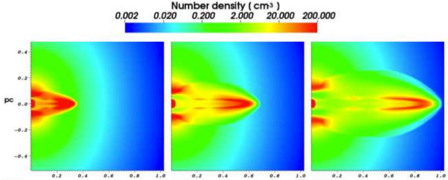

Model 4: toroidal AGB → jet. Time={2347, 4753, 7260} yr, from left to right.

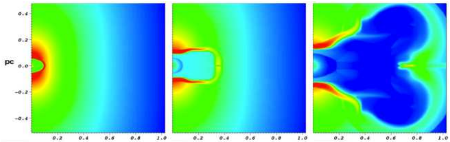

Model 5: toroidal AGB → fast wind. Time={1319, 2618, 3918} yr, from left to right.

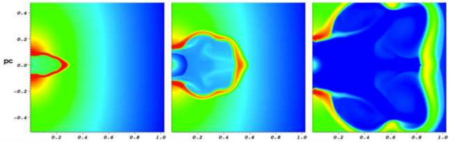

Model 6: toroidal AGB → jet → fast wind. Time={1855, 3806, 6190} yr, from left to right.

Evolution of the gas starting with a spherical (left) or toroidal (right) AGB wind density distribution.

The Interaction of Asymptotic Giant Branch Stars with the Interstellar Medium

E.Villaver, A. Manchado, G. García-Segura (2012)

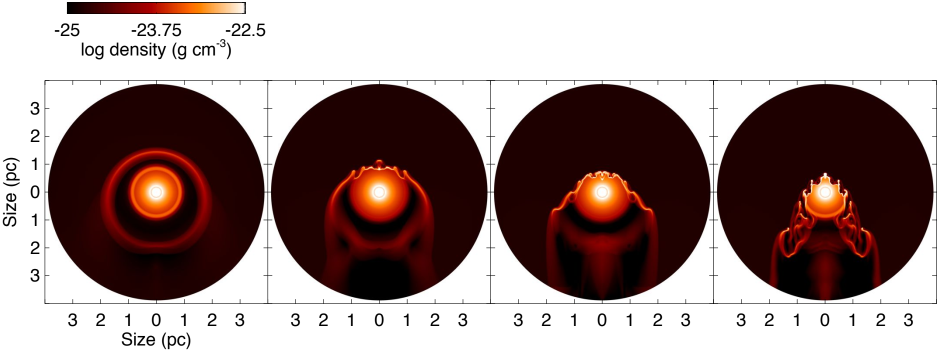

Snapshots taken at 4.74×10^5yr *of a* $1\ M_\odot$ *star moving (from left to right) at 10, 30, 50, 100* $\mathrm{km\,s^{-1}}$. *ISM density is* $0.1\ cm^{-3}$. *As the relative velocity of the star with respect to the ISM increases, the opening angle of the bow shock decreases, the effect of instabilities in the shell morphology and the cometary tail in the downward direction become more prominent.*

Outline

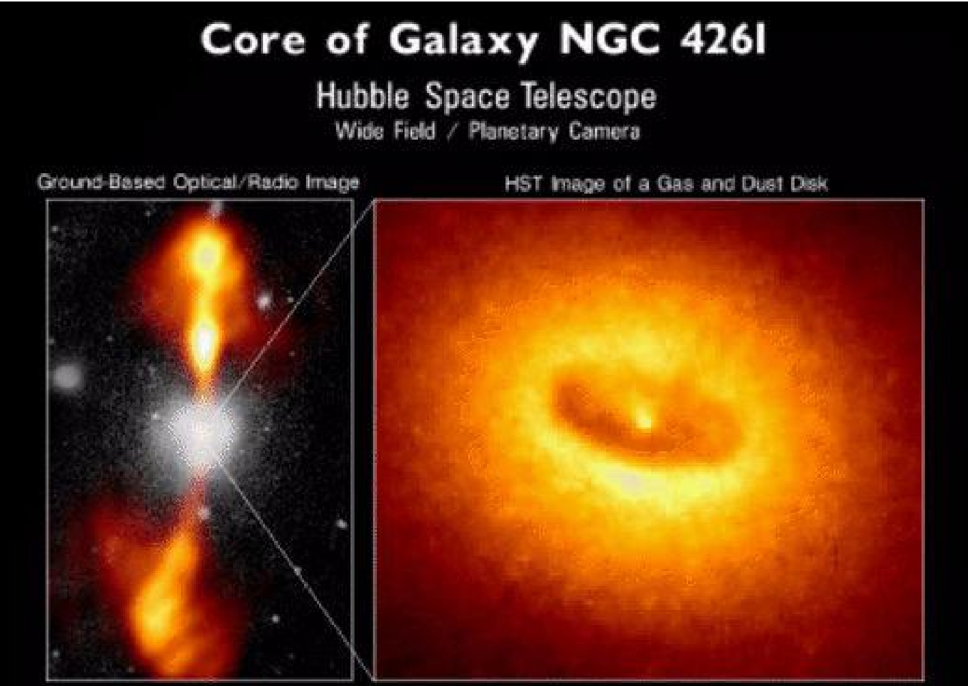
Core of Galaxy NGC 4261
Hubble Space Telescope
Wide Field / Planetary Camera
Ground-Based Optical/Radio Image
HST Image of a Gas and Dust Disk

Einstein's world: Special Relativity vs General Relativity

Special-Relativistic Hydrodynamics *(SRHD)*: $\mathbf{v} \to \mathbf{c} \quad (\mathbf{c} = 1)$

- **Relativistic Jets**: *AGNs, GRBs, microQSOs*

General-Relativistic Hydrodynamics *(GRHD)*: $\mathbf{R} \to \frac{\mathbf{2GM}}{\mathbf{c^2}} \quad (\mathbf{G} = \mathbf{c} = \mathbf{1})$

- **Stellar Core Collapse**: *Hydrodynamical SNe (SNIb/c, SNII), NS/BH formation*
- **Tidal Disruption by a SMBH**: *SNIa-like (WD)*
- **Coalescing Compact Binaries**: *NS-NS, WD-NS, WD-WD, NS-BH*
- **Progenitors of lGRBs**: *Collapsars*
- **Progenitors of sGRBs**: *Mergers of (magnetized-) NS-NS*
- **(Relativistic-) Jet Formation**: *Accretion torus around BHs, ...*

SRHD $\subset$ GRHD

Outline

Structure and dynamics of (classical) supersonic jets *Norman, Winkler, Smarr, Smith (1982)*

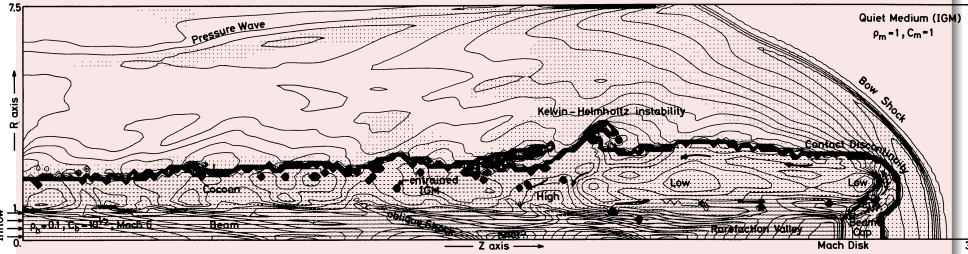

Density contours of a hot $(\rho_b = 0.1)$*, Mach 6 jet. Velocity vectors are drawn at every grid-point. Beam gas is admitted at the lower left-hand corner with velocity 19, which streams to the right where it is shock decelerated and heated at the Mach disk. The working surface moves forward with velocity 4.2, setting up a bow shock in the IGM. High pressure beam cap gas flows first laterally and then back along the beam to feed the cocoon . Structural changes near the beam cap perturb the contact discontinuity; perturbations grow via the Kelvin-Helmholtz instability as they advect back along the jet. Perturbations transmitted to the beam by the cocoon set up oblique internal shock waves.*

Structure and dynamics of (classical) supersonic jets *Norman, Winkler, Smarr, Smith (1982)*

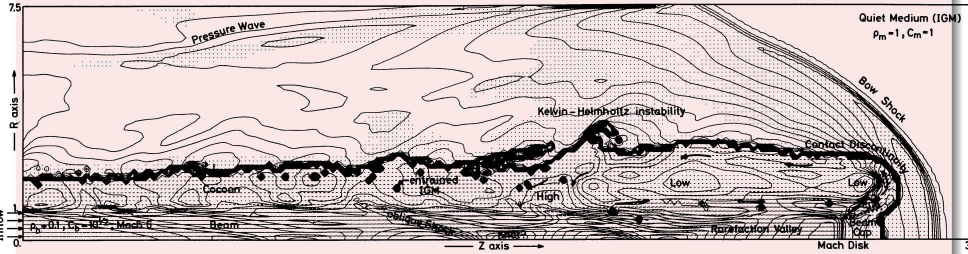

Density contours of a hot $(\rho_b = 0.1)$*, Mach 6 jet. Velocity vectors are drawn at every grid-point. Beam gas is admitted at the lower left-hand corner with velocity 19, which streams to the right where it is shock decelerated and heated at the Mach disk. The working surface moves forward with velocity 4.2, setting up a bow shock in the IGM. High pressure beam cap gas flows first laterally and then back along the beam to feed the cocoon . Structural changes near the beam cap perturb the contact discontinuity; perturbations grow via the Kelvin-Helmholtz instability as they advect back along the jet. Perturbations transmitted to the beam by the cocoon set up oblique internal shock waves.*

Why Ultrarelativistic Numerical Hydrodynamics is difficult? *Norman & Winkler* *(Workshop on Astrophysical Radiation Hydrodynamics, Garching, 1982; Proc. published by Kluwer, 1986)*

WHY ULTRARELATIVISTIC NUMERICAL HYDRODYNAMICS IS DIFFICULT

Michael L. Norman and Karl-Heinz A. Winkler

Los Alamos National Laboratory
and
Max-Planck-Institut fuer Physik und Astrophysik

ABSTRACT

WHY ULTRARELATIVISTIC NUMERICAL HYDRODYNAMICS IS DIFFICULT 471

In multidimensions, a number of avenues need to be explored. As pointed out in the introduction, we consider Lagrangean techniques unsuitable for modeling relativistic flows of astrophysical interest because of the unavoidable shear-induced mesh tangling difficulties.

Under the category of explicit Eulerian techniques, we need to investigate the application to relativistic hydrodynamics of new algorithms which handle shock fronts without artificial viscosity, such as Woodward's Piecewise Parabolic Method (Woodward, this volume). Gone are the difficulties of self-consistently incorporating Q into the difference equations and solving them. But what new dif-

General Relativistic Hydrodynamics (GRHD): *Characteristic structure*

3+1 Formalism: *Darmois (1927), Lichnerowicz (1939), Choquet-Bruhat (1948), Arnowitt, Deser & Misner (1962), York (1979)*

$$ds^2 = -\alpha^2 dt^2 + \gamma_{ij}(dx^i + \beta^i dt)(dx^j + \beta^j dt)$$

Geometrical (dynamical) quantities:

$*$ lapse function: α

$*$ shift vector: β^i

$*$ three-metric: γ_{ij}

Minkowski space-time (Cartesian coordinates):

$\alpha = 1, \beta^i = 0\ , \gamma_{ij} = \delta_{ij}$.

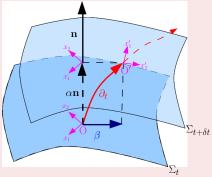

GRHD: The equations (perfect fluid)

- $\mathbf{T^{\mu\nu} = (\rho(1+\varepsilon) + p)\, u^\mu u^\nu + g^{\mu\nu} p}$

u^μ is the four-velocity, ρ the proper rest mass density, ε the specific internal energy, p the pressure

- Local Conservation Laws:

Mass: $\nabla_\alpha(\rho \mathbf{u}^\alpha) = \mathbf{0}$

Energy-Momentum: $\nabla_\alpha \mathbf{T}^{\alpha\beta} = \mathbf{0}$

EOS: $p = p(\rho, \varepsilon)$

General Relativistic Hydrodynamics (GRHD): *Characteristic structure*

3+1 Formalism: *Darmois (1927), Lichnerowicz (1939), Choquet-Bruhat (1948), Arnowitt, Deser & Misner (1962), York (1979)*

$$ds^2 = -\alpha^2 dt^2 + \gamma_{ij}(dx^i + \beta^i dt)(dx^j + \beta^j dt)$$

Geometrical (dynamical) quantities:

$*$ lapse function: α

$*$ shift vector: β^i

$*$ three-metric: γ_{ij}

Minkowski space-time (Cartesian coordinates):

$\alpha = 1, \beta^i = 0$, $\gamma_{ij} = \delta_{ij}$.

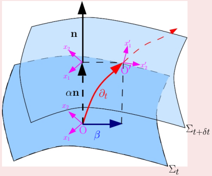

GRHD: The equations (perfect fluid)

- $\mathbf{T^{\mu\nu} = (\rho(1+\varepsilon) + p)\, u^\mu u^\nu + g^{\mu\nu} p}$

u^μ is the four-velocity , ρ the proper rest mass density , ε the specific internal energy , p the pressure

- Local Conservation Laws:

Mass:	Energy-Momentum:	EOS:
$\nabla_\alpha(\rho \mathbf{u}^\alpha) = \mathbf{0}$	$\nabla_\alpha \mathbf{T}^{\alpha\beta} = \mathbf{0}$	$p = p(\rho, \varepsilon)$

GRHD: The Conserved Variables

Martí, Ibáñez & Miralles (1991), Banyuls, Font, Ibáñez, Martí & Miralles (1997)

$$D = \rho W$$
$$S^i = \rho h W^2 v^i$$
$$\tau = \rho h W^2 - p - D$$

$v^i = u^i/(\alpha u^0) + \beta^i/\alpha$ three-velocity

$W = 1/\sqrt{1 - \gamma_{ij} v^i v^j}$ Lorentz factor

$h = 1 + \epsilon + p/\rho$ specific enthalpy

GRHD equations as a HSCL

Conserved quantities: $\mathbf{F^0} = (\mathbf{D}, \mathbf{S^i}, \tau)$

$$\boxed{\frac{1}{\sqrt{-g}}\left[\frac{\partial\sqrt{\gamma}\mathbf{F^0}}{\partial x^0} + \frac{\partial\sqrt{-g}\mathbf{F^i}}{\partial x^i}\right] = \mathbf{S}}$$

$\mathbf{F^i}$ are the fluxes, and $\mathbf{S}$ the sources ($g = \det g_{\mu\nu}$, $\gamma = \det \gamma_{ij}$).

GRHD Equations as a HSCL *Banyuls, Font, Ibáñez, Martí & Miralles (1997)*

$$\frac{1}{\sqrt{-g}}\left(\frac{\partial\sqrt{\gamma}\rho W}{\partial t}+\frac{\partial\sqrt{-g}\rho W v^i}{\partial x^i}\right) = 0$$

$$\frac{1}{\sqrt{-g}}\left(\frac{\partial\sqrt{\gamma}\rho h W^2 v^j}{\partial t}+\frac{\partial\sqrt{-g}(\rho h W^2 v^i v^j + P\delta^{ij})}{\partial x^i}\right) = \mathcal{S}_M^j$$

$$\frac{1}{\sqrt{-g}}\left(\frac{\partial\sqrt{\gamma}(\rho h W^2 - P - \rho W)}{\partial t}+\frac{\partial\sqrt{-g}(\rho h W^2 - \rho W)v^i}{\partial x^i}\right) = \mathcal{S}_E$$

$$\mathcal{S}_M^j = T^{\mu\nu}\gamma^{jk}\left(\frac{\partial g_{\nu k}}{\partial x^\mu} - \Gamma^\eta_{\mu\nu} g_{\eta k}\right)$$

$$\mathcal{S}_E = \alpha\left(T^{\mu 0}\frac{\partial \ln\alpha}{\partial x^\mu} - T^{\mu\nu}\Gamma^0_{\mu\nu}\right) \quad , \quad \Gamma^\lambda_{\mu\nu} \rightarrow Christoffel\ \ symbols$$

SRHD equations: $\eta_{\mu\nu} = (-1,+1,+1,+1)$

$$\frac{\partial\rho W}{\partial t}+\frac{\partial\rho W v^i}{\partial x^i} = 0$$

$$\frac{\partial\rho h W^2 v^j}{\partial t}+\frac{\partial(\rho h W^2 v^i v^j + P\delta^{ij})}{\partial x^i} = 0$$

$$\frac{\partial(\rho h W^2 - P - \rho W)}{\partial t}+\frac{\partial(\rho h W^2 - \rho W)v^i}{\partial x^i} = 0$$

Classical limit

$$\frac{\partial\rho}{\partial t}+\frac{\partial\rho v^i}{\partial x^i} = 0$$

$$\frac{\partial\rho v^j}{\partial t}+\frac{\partial(\rho v^i v^j + P\delta^{ij})}{\partial x^i} = 0$$

$$\frac{\partial(\rho\epsilon + \frac{1}{2}\rho v^2)}{\partial t}+\frac{\partial(\rho\epsilon + \frac{1}{2}\rho v^2 + P)v^i}{\partial x^i} = 0$$

Exact Solution of the Riemann Problem in RHD *Martí & Müller (1994)*

- Riemann problem:
  IVP with initial discontinuous data L, R.

- Self-similar solution:

$$LR \rightarrow \; L\,\mathcal{W}_{\leftarrow}\; L_*\;\mathcal{C}\;R_*\;\mathcal{W}_{\rightarrow}\;R$$

  $\mathcal{W}$ denotes a shock (discontinuos solution) or a rarefaction (selfsimilar expansion),
  and $\mathcal{C}$, a contact discontinuity

- The compressive character of shock waves allows us to discriminate between shocks ($\mathcal{S}$) and rarefaction waves ($\mathcal{R}$):

$$\mathcal{W}_{\leftarrow\,(\rightarrow)} = \begin{cases} \mathcal{R}_{\leftarrow\,(\rightarrow)} & , \quad p_b \leq p_a \\ \mathcal{S}_{\leftarrow\,(\rightarrow)} & , \quad p_b > p_a \end{cases}$$

  where p is the pressure and subscripts a and b denote quantities ahead and behind the wave.

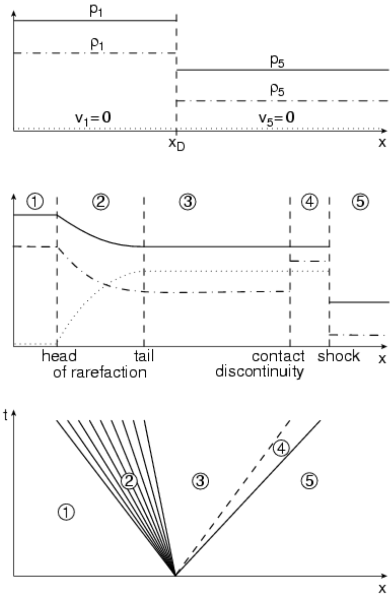

Testing a RHD-code based on Riemann Solvers *Martí & Müller (2003)*

Relativistic reflection shock

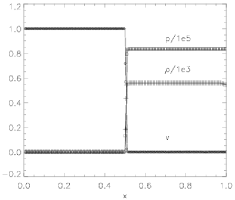

Third-order scheme, perfect fluid EOS ($\gamma = 5/3$), $\Delta x = 1/400$ $v_1 = 0.99999c$ ($W_1 = 224$)

Relativistic Sod's problem

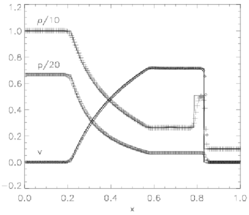

Third-order scheme, perfect fluid EOS ($\gamma = 5/3$), $\Delta x = 1/200$

Relativistic blast wave

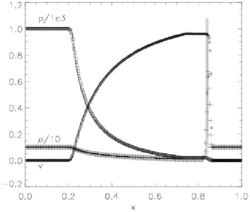

Third-order scheme, perfect fluid EOS ($\gamma = 5/3$), $\Delta x = 1/400$

(i) Stable and sharp discrete shock profiles. **(ii) Accurate propagation speed of discontinuities.**

Relativistic Emery's step

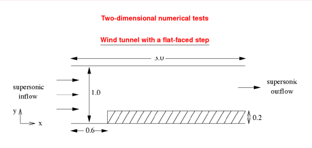

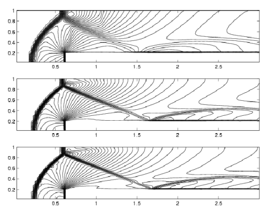

Solution of the Riemann Problem in RHD (tangential velocities) *Pons, Martí & Müller (2000)*

Intrinsic relativistic effects
⇕
Coupling of tangential speeds

- In RHD, all the components of the flow velocity are coupled, through the Lorentz factor, in the solution of the Riemann problem.
- In adition, the specific enthalpy also couples with the tangential velocities $\Longrightarrow$ Important in the thermodynamically ultrarelativistic regime
- Two FORTRAN programs (**RIEMANN, RIEMANN-VT**) are provided by Martí, & Müller, **www.livingreviews.org/lrr-2003-7** $\Longrightarrow$ To compute the *exact solution of an arbitrary special relativistic Riemann problem* for an ideal gas (constant adiabatic index), both with zero and non-zero tangential speeds.

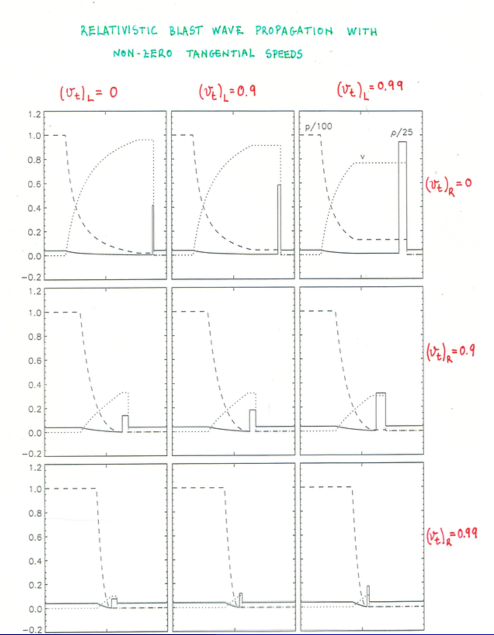

sGRBs: relativistic effects induced by tangential velocities Aloy & Rezzolla (2006)

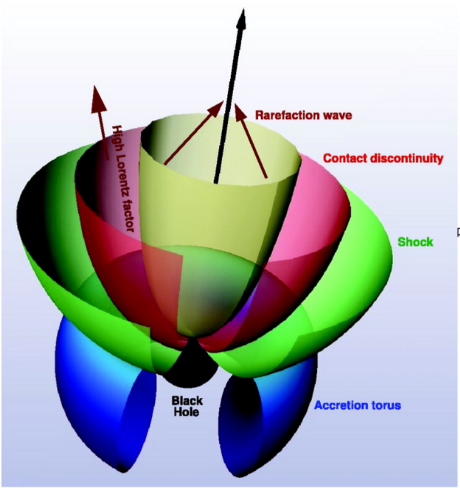

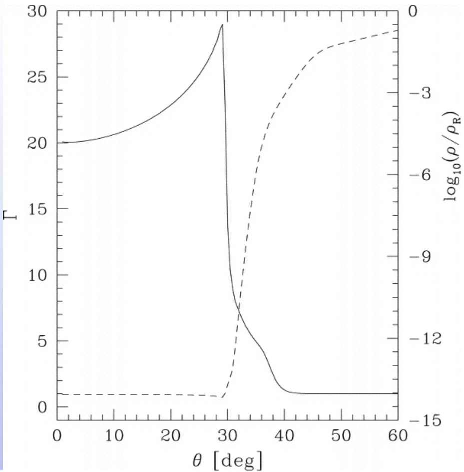

There is a purely relativistic chanel to transform enthalpy into LF $\longrightarrow$ Hydrodynamical boost of flows in the outer layers of jets and GRBs.

Left.- Schematic flow structure of a sGRB produced by an accretion torus orbiting around a stellar-mass BH. The arrows mark the direction of fluid velocity at the rarefaction head (yellow surface), indicating that collimation of the fluid tends towards the BH rotation axis (black arrow). A large boost is produced in the region between the rarefaction head and the contact discontinuity (red surface) separating the relativistic outflow from the shocked external medium.

Right.- Example of the growth of the LF from a multidimensional simulations of ultrarelativistic jets generated in post-neutron star mergers.

General Relativistic Magnetohydrodynamics (GRMHD): Equations *Anile A.M. (1989)*

Definitions

$$T^{\mu\nu} = T^{\mu\nu}_{\text{pf}} + \frac{1}{2} b^\alpha b_\alpha g^{\mu\nu} - b^\mu b^\nu$$

$$T^{\mu\nu}_{pf} = (\rho(1+\varepsilon) + p)\, u^\mu u^\nu + g^{\mu\nu} p$$

ρ: proper rest mass density, ε: specific internal energy, p: pressure

$$h^* = 1 + \varepsilon + \frac{p^*}{\rho} \ , \ p^* = p + \frac{|b|^2}{2}$$

$$H^{\mu\nu} = u^\mu b^\nu - u^\nu b^\mu \ , \ u^\mu = W(1, v^x, v^y, v^z)$$

$b^\mu = (b^0, b^x, b^y, b^z)$, $b_\mu b^\mu = | b |^2 \geq 0$, where

$$b^\mu = \left(\frac{W B_k v^k}{\alpha}, \frac{B^i}{W} + W B_k v^k (v^i - \frac{\beta^i}{\alpha}) \right)$$

GRMHD: The Equations

Conservation of mass: $\nabla_\alpha (\rho u^\alpha) = 0$

Conservation of energy and momentum:

$$\nabla_\alpha T^{\alpha\beta} = 0$$

Maxwell Equations: $\nabla_\mu H^{\mu\nu} = 0$

Induction equation: $\nabla_\alpha (u^\alpha b^i - u^i b^\alpha) = 0$

$\left(\Rightarrow \frac{\partial \mathbf{B}}{\partial t} - \nabla \times (\mathbf{v} \times \mathbf{B}) = 0\right)$

Differential constraint on the initial magnetic field configuration:

$\partial_\alpha (u^\alpha b^0 - u^0 b^\alpha) = 0 \ (\Rightarrow \nabla \cdot \mathbf{B} = 0)$

Algebraic constraints: $u^\alpha u_\alpha = -1$, $u^\alpha b_\alpha = 0$

Equation of state: $p = p(\rho, \varepsilon)$ $[p = (\gamma - 1)\rho\varepsilon]$

GRMHD equations as a HSCL: Conserved variables (U), fluxes (F) and sources (S)

Antón, Zanotti, Miralles, Martí, Ibáñez, Font, Pons (2006)

$$\frac{1}{\sqrt{-g}} \frac{\partial \sqrt{\gamma}\, \mathbf{U}}{\partial t} + \frac{1}{\sqrt{-g}} \frac{\partial \sqrt{\gamma}\, \mathbf{F^i}}{\partial x^i} = \mathbf{S} \quad \text{and} \quad \frac{\partial \sqrt{\gamma}\, B^i}{\partial x^i} = 0$$

$$\mathbf{U} = \begin{pmatrix} \rho W \\ (\rho h + b^2) W^2 v_j - \alpha b^0 b_j \\ (\rho h + b^2) W^2 - \left(p + \frac{1}{2} b^2\right) - (\alpha b^0)^2 \\ B^k \end{pmatrix}$$

$$\mathbf{F^i} = \begin{pmatrix} \rho W (v^i - \frac{\beta^i}{\alpha}) \\ (\rho h + b^2) W^2 v_j (v^i - \frac{\beta^i}{\alpha}) + \left(p + \frac{1}{2} b^2\right) \delta^i_j - b^i b_j \\ (\rho h + b^2) W^2 (v^i - \frac{\beta^i}{\alpha}) - \alpha b^0 b^i - \left(p + \frac{1}{2} b^2\right) \frac{\beta^i}{\alpha} \\ B^i (\alpha v^k - \beta^k) - B^k (\alpha v^i - \beta^i) \end{pmatrix}$$

$$\mathbf{S} = \begin{pmatrix} 0 \\ T^{\mu\nu} \left(\partial_\mu g_{\nu j} - \Gamma^\delta_{\mu\nu} g_{\delta j}\right) \\ \alpha \left(T^{\mu 0}\, \partial_\mu \log \alpha - T^{\mu\nu}\, \Gamma^0_{\mu\nu}\right) \\ 0^k \end{pmatrix}$$

RMHD: Exact Riemann Solver (Transversal Field) *Romero, Martí, Pons, Ibáñez, Miralles (2005)*

An exact (magneto-)shock-tube test

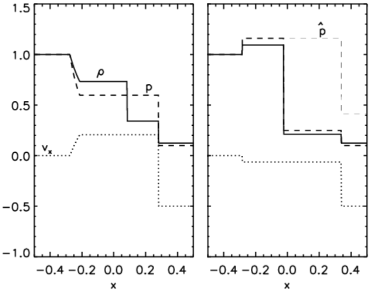

Solution of the Riemann problem ($t = 0.4$)

$p_L = 1.0$, $\rho_L = 1.0$, $v^x_L = 0.0$;
$p_R = 0.1$, $\rho_R = 0.125$, $v^x_R = -0.5$

Ideal gas EOS ($\gamma = 5/3$)

(Left) **A purely hydrodynamical problem**

(Right) **Tangential magnetic field:** $b_R = 2.0$

Analytical Magnetosonic velocities ($\mathbf{u}^\mu \mathbf{b}_\mu = \mathbf{0}$)

$$\boxed{u^\mu = W(1, v^x, 0, v^z) \ , \ b^\mu = (0, 0, b, 0)}$$

$$\lambda_0 = v^x$$

$$\lambda_\pm = \frac{v^x(1-\omega^2) \pm \omega\sqrt{(1-v^2)[1-(v^x)^2 - (v^2-(v^x)^2)\omega^2]}}{1 - v^2\omega^2}$$

$$\omega^2 = c_s^2 + \mathbf{c_a}^2 - c_s^2\mathbf{c_a}^2 \quad , \quad c_a^2 = \frac{|b|^2}{\rho h^*}$$

1D $\Longrightarrow$ $v^z = 0 \to v = v^x$: $\lambda_0 = v$, $\lambda_\pm = \dfrac{v \pm \omega}{1 \pm v\omega}$

¶ $|\lambda_\pm| \geq |\lambda_\pm^{(fms)}|$ *(Leismann, Antón, Aloy, Müller, Martí, Miralles, Ibáñez, 2005)*

The exact solution of the Riemann problem in RMHD, in the general case, has been derived by ***Giacomazzo & Rezzolla, 2006***

Outline

Einstein Equations (3+1 Formalism): $\mathbf{G}^{\mu\nu} = 8\pi\mathbf{T}^{\mu\nu}$

Evolution of geometrical (dynamical) quantities :

$$\partial_t \gamma_{ij} = -2\alpha K_{ij} + \nabla_i \beta_j + \nabla_j \beta_i$$

$$\partial_t K_{ij} = -\nabla_i \nabla_j \alpha + \alpha(R_{ij} + K K_{ij} - 2K_{im}K_j^m) + \beta^m \nabla_m K_{ij} + K_{im}\nabla_j \beta^m + K_{jm}\nabla_i \beta^m - 8\pi T_{ij}$$

$$\bigoplus$$

Constraints:

$$0 = R + K^2 - K_{ij}K^{ij} - 16\pi\alpha^2 T^{00}$$
$$0 = \nabla_i (K^{ij} - \gamma^{ij} K) - 8\pi S^j$$

$R_{\mu\nu}$ the Ricci tensor, R the Riemann scalar, K_{ij} the extrinsic curvature, $K = \gamma^{ij} K_{ij}$

¶ E. Gourgoulhon, J.L. Jaramillo, **A 3+1 perspective on null hypersurfaces and isolated horizons**, Phys.Rept. 423 (2006) 159–383,

Numerical Relativity (NR): *From the Dark Age ('60s) to the Golden Age (2004,...)*

- *Mathematical structure of the PDEs* : hyperbolic, elliptic-hyperbolic

$$\oplus$$

- *Coordinate gauge conditions* : geodesic, maximal, harmonic $('1 + log')$, quasi-isotropic, radial, minimal distortion, Dirac

$$\oplus$$

- *BH Singularity* : Excision, Puncture, Moving punctures

$$\oplus$$

- *Numerics* : Algorithms

$$\oplus$$

- *Supercomputing* : Code programming, AMR, visualization, ...

Numerical Relativity (NR): *From the Dark Age ('60s) to the Golden Age (2004,...)*

- *Mathematical structure of the PDEs* : hyperbolic, elliptic-hyperbolic

$$\oplus$$

- *Coordinate gauge conditions* : geodesic, maximal, harmonic $('1+log')$, quasi-isotropic, radial, minimal distortion, Dirac

$$\oplus$$

- *BH Singularity* : Excision, Puncture, Moving punctures

$$\oplus$$

- *Numerics* : Algorithms

$$\oplus$$

- *Supercomputing* : Code programming, AMR, visualization, ...

NR: The art and science of developing computer algorithms to solve Einstein's equations for astrophysically realistic, high-velocity, strong-field systems. *Baumgarte & Shapiro (2010)*

- Einstein's theory of relativistic gravitation is the cornerstone of modern cosmology, the physics of neutron stars and black holes, the generation of gravitational radiation and countless other cosmic phenomena in which strong-field gravitation plays a dominant role.
- With the advent of supercomputers, it is now possible to tackle these complicated equations numerically and explore these scenarios in detail.

3+1 Formalism: Formulations of Einstein Equations (*BSSN, FCF, ...)*

Free evolution scheme: Solving the constraint equations only to get the initial data.

- **BSSN**: **Shibata & Nakamura, 1995; Baumgarte & Shapiro, 1999.**
  - **Much improved stability with respect to the standard ADM formulation.**
  - **Rigurous mathematical analysis (well-posedness, symmetric hyperbolic,...)** *Gundlach & Martín-Garcia (2004,2005,2006)*
  - **The most successful computations in numerical relativity to date**
    - *Binary neutron stars* **(Shibata and Uryu, 2000, 2001, 2002; Shibata et al., 2003).**
    - *Long-term evolution of neutron stars* **(Font et al. 2002).**
    - *Gravitational collapse of neutron stars to black holes* **(Shibata 2003; Baiotti et al., 2004).**
- **Other First Order Hyperbolic formulations: Reula,** *Hyperbolic Methods for Einstein's Equations*, Living Reviews in Relativity (www.livingreviews.org), 1998. **Bona & Palenzuela-Luque,** *Elements of Numerical Relativity*, Lecture Notes in Physics, v. 673 (2005).

FCF (Fully Constrained Formulation): Solving the four constraint equations at each time step.

Bonazzolla, Gourgoulhon, Grandclément & Novak, 2004 Cordero-Carrión, Ibáñez, Jaramillo, Gourgoulhon & Novak, 2008; Cordero-Carrión, Cerdá-Durán, Dimmelmeier, Jaramillo, Novak & Gourgoulhon, 2009; Cordero-Carrión, Cerdá-Durán & Ibáñez, 2012

- Elliptic equations are much **more stable** than hyperbolic ones.
- **The constraint-violating modes do not exist** by construction.
- The equations describing stationary spacetimes are usually elliptic and are **naturally recovered**
- **Very efficient numerical techniques, based on spectral methods** .
- **CFC** is recovered in a simple way.

FCF: Gravitational waves in dynamical spacetimes with matter content

Cordero-Carrión, Cerdá-Durán, Ibáñez, 2012

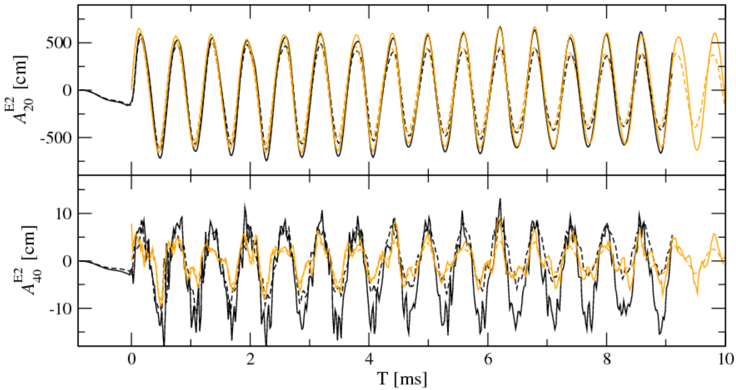

Gravitational wave extracted from simulations of an oscillating neutron star. Upper and lower panels show the quadrupolar and hexadecapolar component respectively. On each panel we compare simulations for regular (dashed lines) and high (solid lines) resolution finite differences grid. The offset-corrected waveform computed with the direct extraction method (black lines) is compared to the PN method (quadrupole and hexadecapole formulae, orange lines).

Outline

NGC6240: A Double Supermassive Black Hole

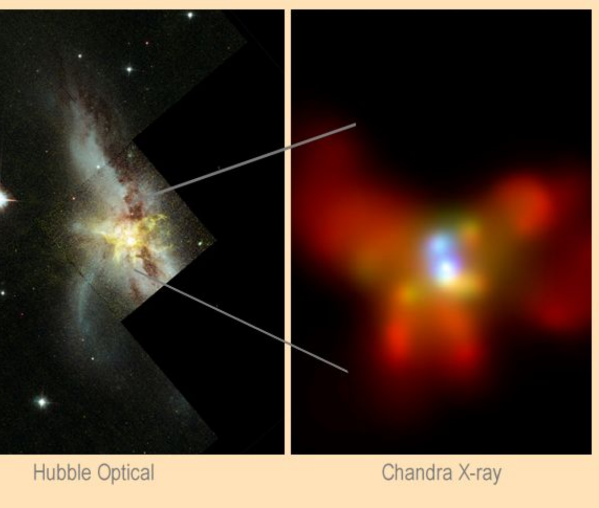

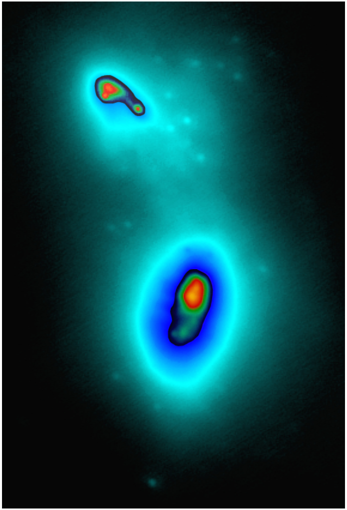

Left. Credits: **Optical**: R.P.van der Marel i J.Gerssen (STScI), NASA; **X-ray**: S.Komossa i G.Hasinger (MPE) et al., CXC, NASA
Right. Keck adaptive optics image of NGC 6240 in K' band. The dark-blue-enclosed regions in the north and south nuclei, which are separated by about 1.6 arcsec, have each been re-scaled to highlight their interior structure. The more diffuse image of the rest of the galaxy's nuclear region uses a logarithmic color map. Many individual young star clusters can be seen exterior to the two nuclei (Pollack, Max, & Schneider, 2007)

BBH simulations: State of the art

1995: Pair of pants
(Head-on collision)

BBH Grand Challenge Alliance

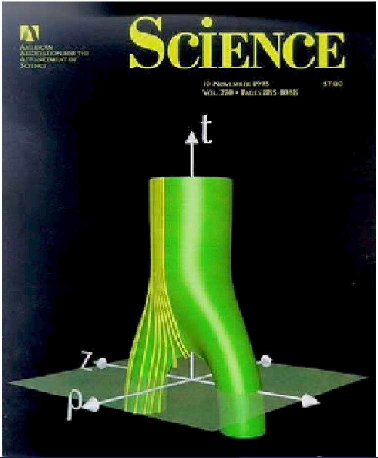

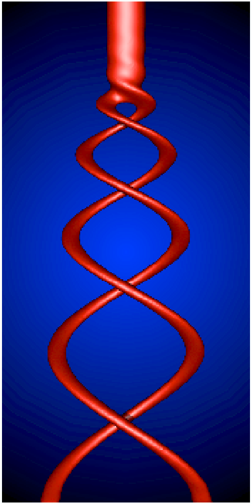

FSU-Jena Numerical Relativity Group

2007: Pair of twisted pants (spiral & merge)

BBH Milestones: *Pretorius, 2005 (top); Campanelli et al., 2006 (bottom)*

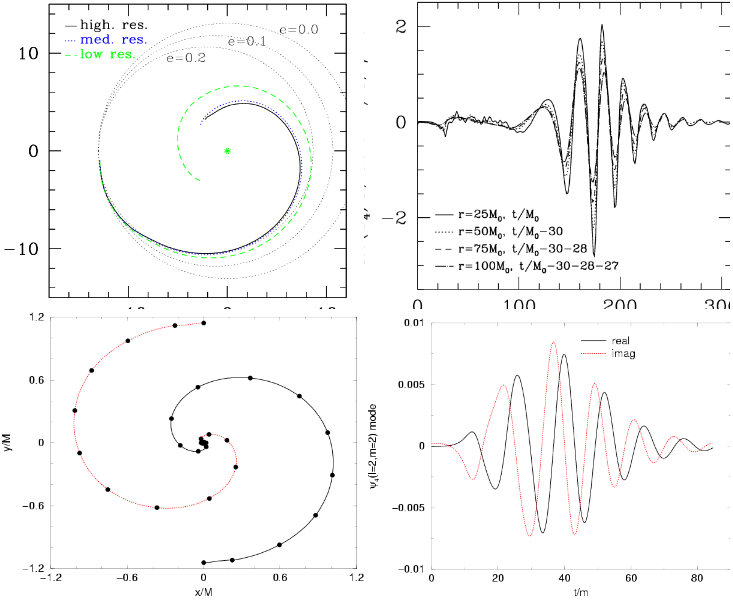

BBH Simulations @ the House of Representatives *(Washington, May 18, 2006)*

May 19, 2006 CONGRESSIONAL RECORD — *Extensions of Remarks* **E885**

(The editorial page at the Times and at some other papers, including The Washington Post, is run by an entirely separate hierarchy that reports directly to the publisher. It is a distinction that remains extremely important to papers where the division is maintained.)

As a manager, Mr. Rosenthal was said to be abrasive and self-centered. A diminutive, bespectacled figure, he had a volcanic temper. Many found him intimidating. He advanced the careers of many journalists and derailed the careers of others. He was a constant source of friction and controversy in the Times newsroom. Admirers and critics spoke of him with equal fervor.

Arthur Gelb, a friend of Mr. Rosenthal's who also was the Times's managing editor, once offered this explanation of the Rosenthal character: ''In every field, in every art, if you talk to an artist who has a very keen mind, you will find they are very restless. Anyone who is truly creative has a restlessness and natural impatience with others.''

There was never any question about Mr. Rosenthal's impact on the Times. He insisted on good writing and sent his reporters on stories that often were ignored by other publications—and might have been missed by the Times except for his guidance.

He expanded coverage in every direction. The religion page, for example, became a venue for discussion of broad theological and philosophical questions rather than a summary of sermons.

Reader-friendly stories and features were added and given prominent display. New emphasis was placed on covering sports and the city itself. The daily paper went from two sections to four. The business report became a separate section. SportsMonday, Weekend and Science Times sections were published on different days of the week. Coverage of topics such as food and the arts was expanded.

At a time when many newspapers in New York and elsewhere in the country were losing readers, the Times's circulation increased and its financial health improved dramatically, due to its expanding national and regional editions.

doing and how he chose to end it. There were other ways he could have ended it—he could have quit!''

In 1971, Mr. Rosenthal played an important role in the Times's publication of the Pentagon Papers, a landmark event in the history of journalism. The papers detailed 25 years of U.S. involvement and deception in Vietnam. The archive of several thousand pages was classified as secret, and the management of the Times expected the government to object to the project.

Mr. Rosenthal, by then the managing editor, put his credibility and career on the line by marshaling the arguments to go ahead anyway. He was supported by then-publisher Arthur Ochs Sulzberger.

On the second day of a planned multipart series, the Justice Department went to court to block publication. There followed two weeks of frantic litigation in courts in New York and Washington and an expedited appeal to the U.S. Supreme Court, in which the Times was joined by The Washington Post. In the end, a divided court affirmed the First Amendment right of the newspapers to bring the information to their readers.

Mr. Rosenthal regarded his greatest contribution to the Times as his effort to keep the news report ''straight.'' By that he meant free of bias and editorializing on the part of reporters.

''I used to tell new reporters: The Times is far more flexible in writing styles than you might think, so don't button up your vest and go all stiff on us,'' he wrote in his farewell column for the Times. ''But when it comes to the foundation—fairness—don't fool around with it, or we will come down on you.''

Mr. Rosenthal gave up the executive editorship of the Times at the end of 1986 and was succeeded by Max Frankel. His first column on the op-ed page appeared Jan. 6, 1987. His last column for the paper was published Nov. 5, 1999.

As a columnist, Mr. Rosenthal's subjects ranged from the evils of the drug trade—''helping make criminals and destroying young minds''—to all forms of political, ethnic and religious repression, from China and

Survivors include his wife of 18 years, the writer Shirley Lord Rosenthal, who lives in Manhattan; three sons from his first marriage, Jonathan Rosenthal of Clifton, Daniel Rosenthal of Milford, N.J., and Andrew Rosenthal, a New York Times deputy editorial page editor who lives in Montclair, N.J.; a sister; and four grandchildren.

UTB'S GRAVITATIONAL WAVE DISCOVERY

HON. SOLOMON P. ORTIZ

OF TEXAS

IN THE HOUSE OF REPRESENTATIVES

Thursday, May 18, 2006

Mr. ORTIZ. Mr. Speaker, I rise today to share with the House a monumental discovery made by scientists in my district that will make it easier for space scientists to map black holes in space. This breathaking discovery on gravitational waves was made by researchers at the University of Texas at Brownsville, and allows scientists—for the first time—to study the warping of space and time produced by colliding black holes.

Now, I'm no rocket scientist—but UTB's gravitational wave studies universal breakthrough will give researchers and other space scientists greater insight into one of the most cataclysmic astrophysical events predicted by Einstein's theory of general relativity, the merger of two black holes. Given that most of us are not scientists, let me just say that this remarkable discovery will guide astrophysicists as they learn more about the origin and history of the supermassive black holes which reside at the core of most galaxies, including our own Milky Way.

Black hole merger models are always challenging to build due to their unique and unknown nature. Black holes in space are regions where gravity is so intense that nothing, including light itself, can evade their pull. Be-

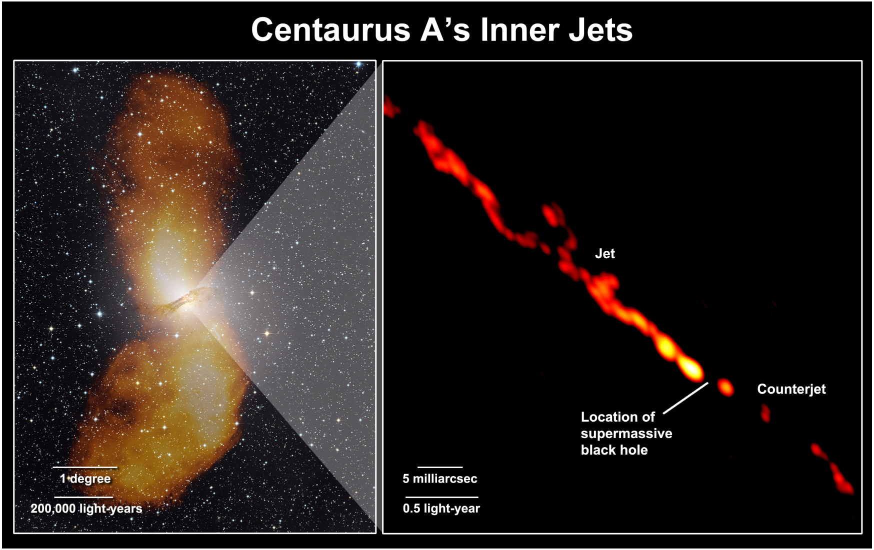

Left: Vast radio-emitting lobes (shown as orange in this optical/radio composite) extend nearly a million light-years from the galaxy. *(Credit: Capella Observatory (optical), with radio data from Feain, Cornwell, and Ekers (CSIRO/ATNF), Morganti (ASTRON), and Junkes (MPIfR)).* *Right:* Radio image from the TANAMI project. This view reveals the inner 4.16 light-years of the jet and counterjet. The image resolves details as small as 15 light-days across. Undetected between the jets is the galaxy's 55-million-solar-mass black hole. *Credit: NASA/TANAMI/Müller et al.*

Astrophysical scenarios governed by relativistic (magneto-)hydrodynamical processes

Relativistic Jets (in AGNs)

- Statistics:
  $\approx$ 10% radio-loud
- $v_{\rm jet}$
  $\approx 0.995c$
- $L_{\rm jet}/L_{\odot}$
  $\approx 10^{10} - 10^{15}$
- Size:
  $\approx 0.1 - 1$ Mpc
- Collimation:
  few degrees
- Central engine:
  SMBH + disc

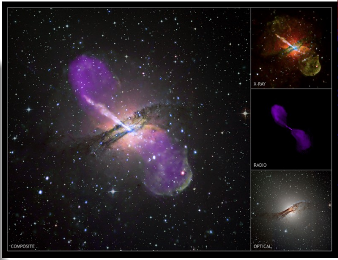

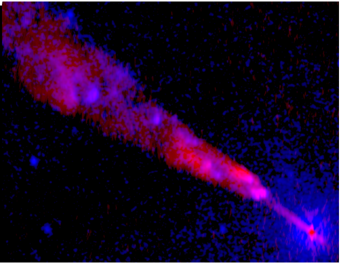


Radio Galaxy 3C219
VLA 20cm image

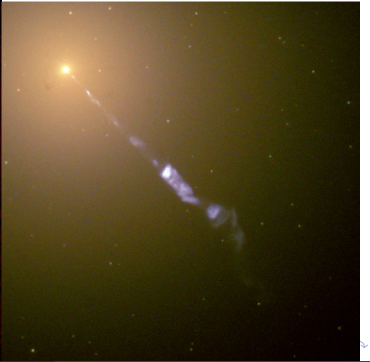

Relativistic Jets in AGNs: Theory versus observations

Jorstad, Marscher, Lister, Stirling, Cawthorne, Gear, Gómez, Stevens, Smith, Forster, Robson, AJ, **130**, 1418 (2005)

- Total and polarized intensity images of 15 AGNs obtained with the VLBA at 7 mm wavelength at 17 epochs from 1998 March to 2001 April. Apparent velocities of 106 features in the jets.

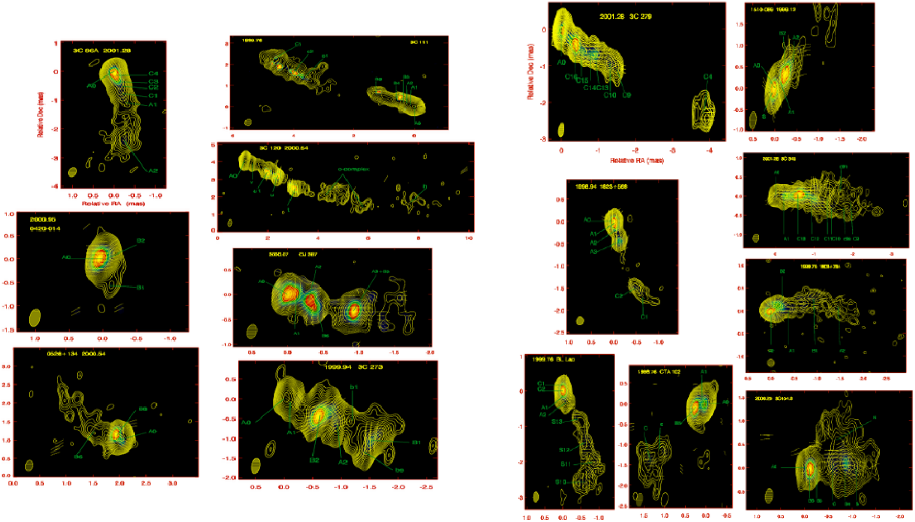

Relativistic Jets in AGNs: Production of Trailing Radio Components

Agudo, Gómez, Martí, Ibáñez, Marscher, Alberdi, Aloy, Hardee (2001); Aloy, Martí, Gómez, Agudo, Müller, Ibáñez (2003)

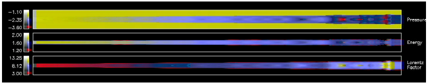

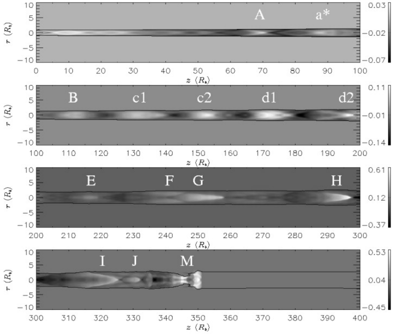

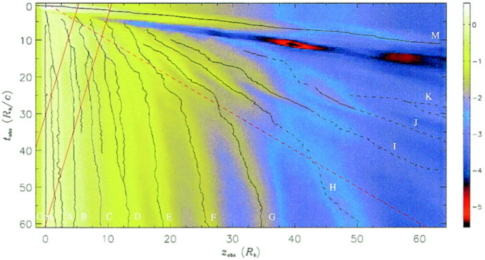

Trailing Shocks: Conical shocks behind strong perturbations

- **Created by the excitation of a local pinch instability. Detected as weak radio components following the main shock**
- ***Left bottom.-* Relative variation with respect to the undisturbed steady jet of the Lorentz factor (logarithmic scale) at t=350 R_b/c. Note the different scale ranges in each frame to enhance the representation of the trailing conical shocks (labeled A to J) following the main perturbation (M). Typical shock angles to the jet axis are $\sim 10 - 15^{\circ}$. (Pressure-matched jet: 400 R_b)**
- **Trailing shocks have distinct properties: i) Created in the wake of strong perturbations. ii) Conical ($\rightarrow$ trace in polarized flux) iii) Flux densities and apparent motions depend strongly on distance from the core at which they are generated (*Right.-* Logarithm of intensity in the OBS frame)**
- **Underlying jet hydrodynamics derived from component spacing, velocity and brightness**
- **DETECTED –for first time – in 3C120 (Gómez et al. 2001)**

Long Term Evolution of Relativistic Jets *Scheck, Aloy, Martí, Müller (2002)*

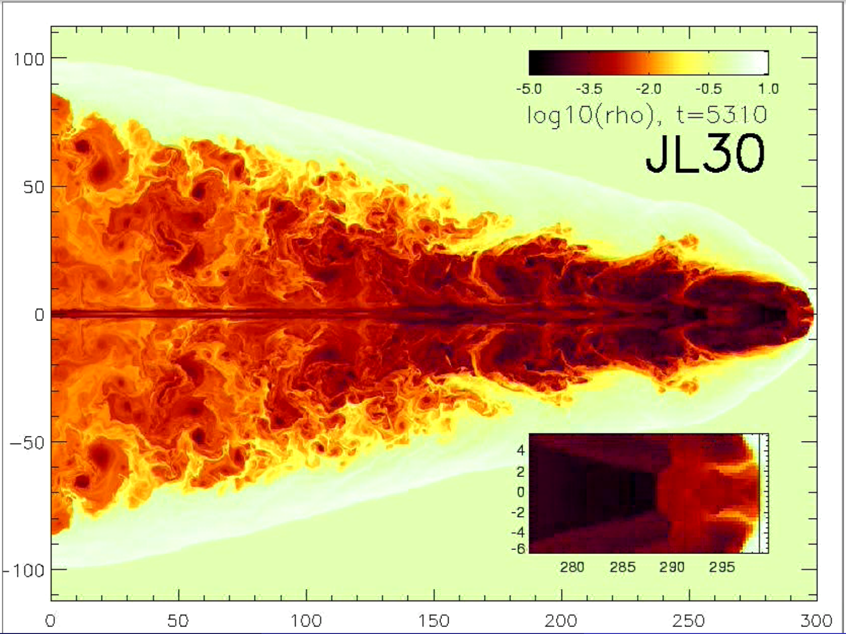

Magnetized Relativistic Jets *Leismann, Antón, Aloy, Müller, Martí, Miralles, Ibáñez (2005)*

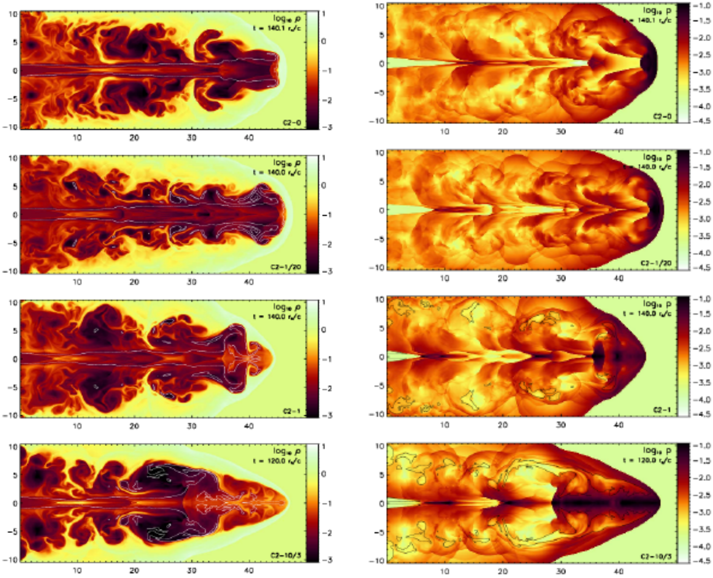

The intensity of the toroidal field increases from top to bottom. Density (*Left*). Pressure (*Right*)

Astrophysical scenarios governed by relativistic (magneto-)hydrodynamical processes

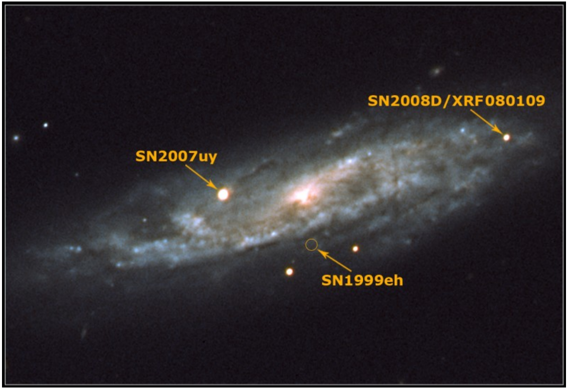

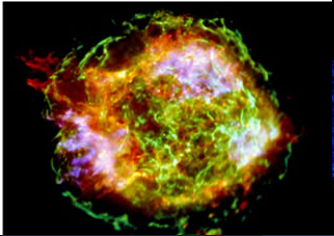

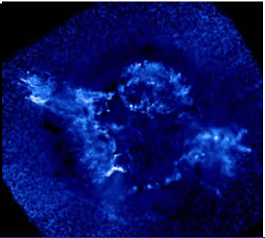

Hydrodynamical Supernovae: SNII, SNIb/c

Top. The spiral galaxy NGC 2770. The three supernovae, indicated in this image, are now thought to be hydrodynamical (core-collapse), but the most recent of the trio, SN2008D, was first detected by the Swift satellite at more extreme energies as an X-ray flash (XRF) or possibly a low-energy version of a gamma-ray burst on January 9th. Located a mere 90 million light-years away in the northern constellation Lynx. (A. de Ugarte Postigo et al., 2007)

Bottom. False-colour image highlighting the jet and counterjet of silicon atoms around the SNR CasA (Hwang et al., 2004)

Structure of the stalled SN shock: Entropy maps, *2D (bottom) vs 3D (top)*

Burrows, Dolence, Murphy, Almgren & Nordhaus (2012)

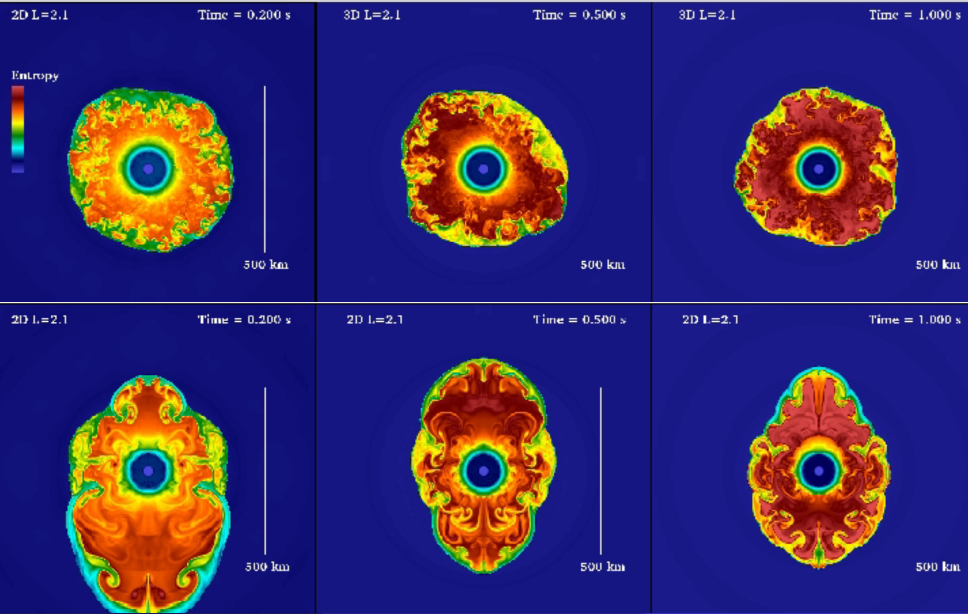

Structure of the stalled SN shock: Entropy maps, *with (up) and without (bottom) neutrino heating*

Burrows, Dolence, Murphy, Almgren & Nordhaus (2012)

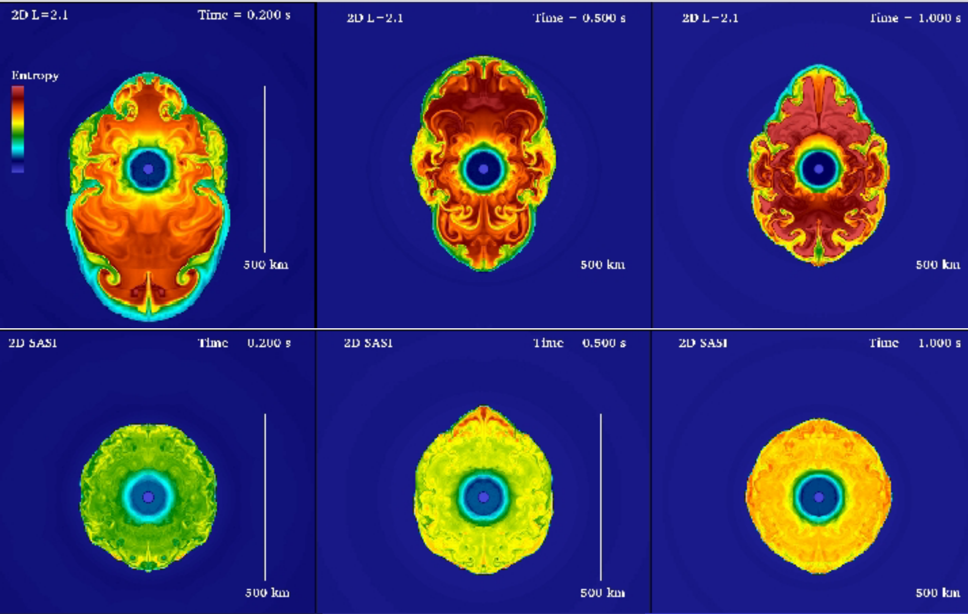

The Dominance of Neutrino-Driven Convection in Core-Collapse Supernovae

Murphy, Dolence & Burrows (2012)

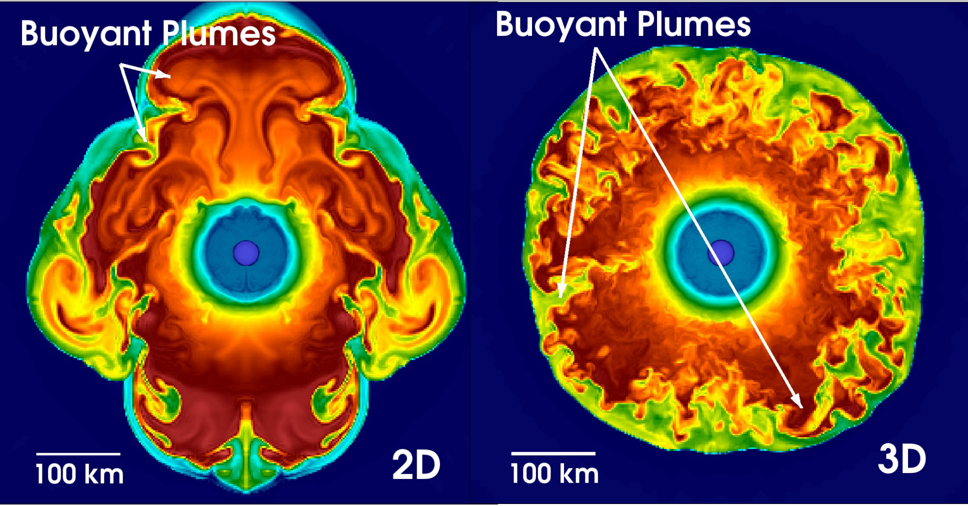

Entropy color maps of 2D (left) and 3D (right) CCSN simulations. Snapshots at 250 ms after bounce for $L_\nu = 2.1 \times 10^{52}$ erg/s. The 2D simulation has a higher proportion of coherent structures, which turbulence theory predicts. Despite the differences between 2D and 3D, both show positively (high entropy) and negatively (low entropy) buoyant plumes, a strong indication of neutrino-driven convection.

Magnetorotational core collapse *Obergaulinger, Aloy, Müller, A&A, **450**, 1107 (2006); Obergaulinger, Aloy, Dimmelmeier, Müller, A&A, **457**, 209 (2006)*

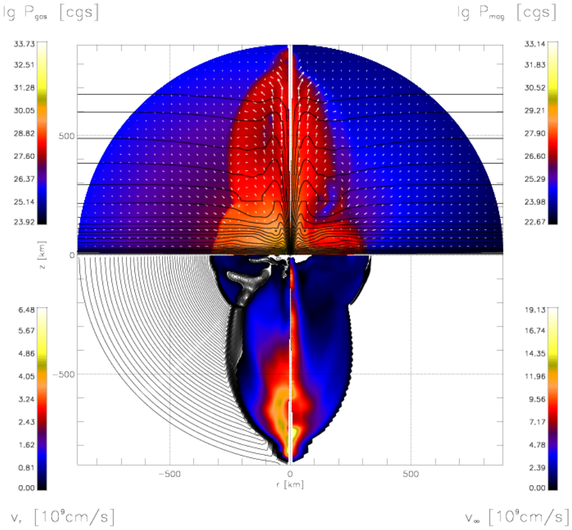

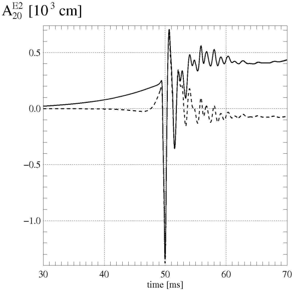

- *A complete parameter set up* ($>$ 50 *models).*
- *Dynamical development of strong magnetic fields (MRI).*
- *New types of GW signals related with the presence of the magnetic field* $\Longrightarrow$ *signatures of the production of jets.*

Magneto-rotational Instability in Core-Collapse Supernovae

Obergaulinger, Cerdá-Durán, Müller & Aloy (2009, 2010)

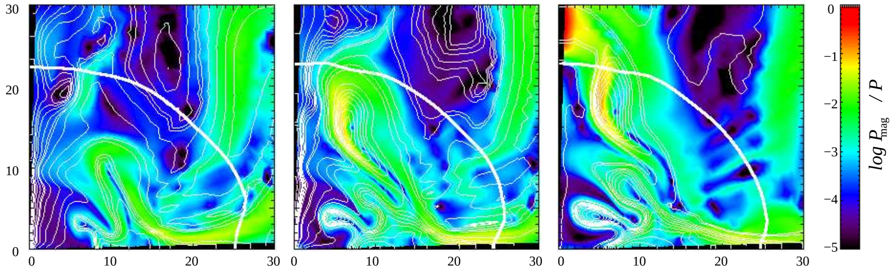

Three snapshots of the innermost 30 km in the post-bounce evolution of a magnetorotational stellar core collapse simulation. Color coded in the logarithm of the ratio of magnetic pressure to thermal pressure. Thin lines indicate magnetic field lines, and thick white line the position of the neutrino-sphere. The elongated structures inside the Proto-Neutron star are channel flows, a distinctive feature of the growth of the magneto-rotational instability.

Gravitational Waves from Core Collapse Supernovae (simplified EoS)

Historical achievements

- **Müller, 1982** $\Longrightarrow$ **2D Newtonian. First numerical evidence of the low gravitational efficiency ($E < 10^{-6} M c^2$) of the core-collapse scenario.**
- **Finn & Evans, 1990** $\Longrightarrow$ **Confirmed Müller's results. Improved quadrupole formula.**
- **Bonazzola & Marck, 1993** $\Longrightarrow$ **First 3D simulations using pseudospectral methods, very accurate and free of numerical or intrinsic viscosity. They found that, still, low amount of energy is radiated in gravitational waves, regardless of whether the initial conditions of the collapse are axisymmetric, rotating or tidally deformed**
- **Zwerger & Müller, 1997** $\Longrightarrow$ **2D Newtonian. Rotating stellar cores.**
- **Rampp, Müller & Ruffert, 1998** $\Longrightarrow$ **3D Newtonian. Rapidly-rotating core-collapse, focusing on non-axisymmetric instabilities**

Zwerger & Müller's catalogue of wave-forms (1997)

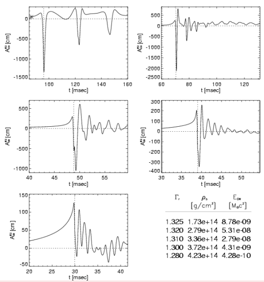

Γ_r	ρ_b [g/cm³]	E_{gw} [$M_\odot c^2$]
1.325	1.73e+14	8.78e-09
1.320	2.79e+14	5.31e-08
1.310	3.36e+14	2.79e-08
1.300	3.72e+14	4.31e-09
1.280	4.23e+14	4.28e-10

Dimmelmeier, Font & Müller, 2001,2002

- *First relativistic attempt. 2D axisymmetric simulations with CFC metric (Isenberg, Wilson & Mathews).* $\Longrightarrow$ **CoCoA code**
- **To extend Newtonian simulations** $\Longrightarrow$ **To determine whether GR effects make a difference in overcoming the angular momentum threshold.**
- **To extract gravitational radiation from core collapse and more realistic waveforms .**
- **To develop a versatile and extensible code for simulating highly relativistic rotating stars .**

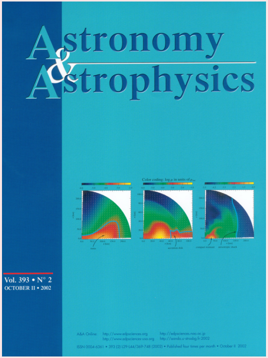

Rotational Core Collapse: DFM's catalogue of wave-forms *Dimmelmeier, Font & Müller (2002)*

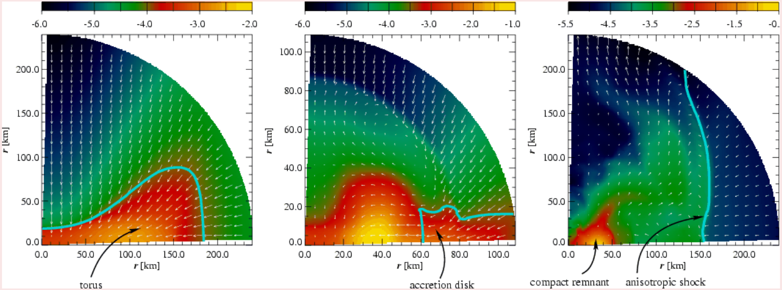

Formation of a torus and shock-propagation in the very rapidly and highly differentially rotating model A4B5G5. The three snapshots show color coded contour plots of the density, $(\log\ \rho,$ **scaled to nuclear matter density), together with the meridional flow field during the infall phase at** $t = 25.0$ ms **(left panel), shortly before the centrifugal bounce at** $t = 31.2$ ms **(middle panel), and at** $t = 35.0$ ms **(right panel).**

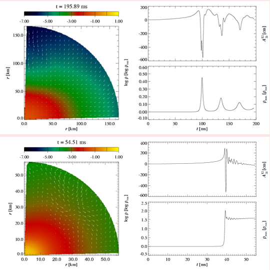

(*Top*) Model A2B4G1 (*Bottom*) Model A3B2G4

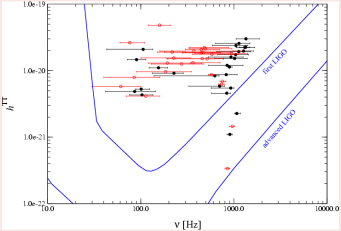

Prospects of detection of the gravitational wave signal from axisymmetric rotational supernova core collapse in relativistic (black filled circles) and Newtonian (red unfilled circles) gravity (D = 10 kpc). 26 models.

Gravitational Waves from Core Collapse Supernovae (realistic EoS)

Dimmelmeier, Ott, Janka, Marek & Müller; Ott, Dimmelmeier, Marek, Janka, Hawke, Zink & Schnetter (2007)

Catalogue of wave-forms: Rotation

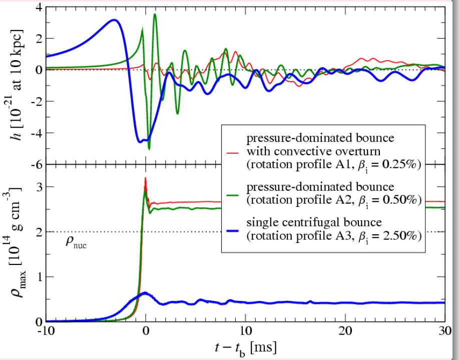

Time evolution of the GW amplitude h and maximum density ρ_{max} for three representative models with different rotation profiles and initial rotation rates. The gravitational wave burst signals from the core bounce are generic, known as Type I.

Catalogue of wave-forms: 2D vs 3D

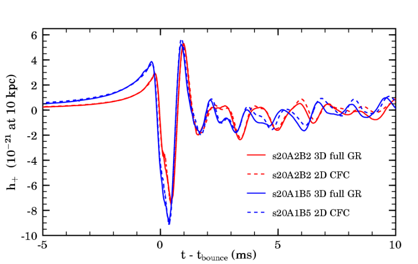

GW strain h_+ along the equator for models s20A2B2 and s20A1B5. 2D-CFC and 3D-full-GR results are compared.

Three-dimensional relativistic simulations of rotating neutron star collapse to a Kerr BH

Baiotti, L., Hawke, I., Montero, P.J., Loeffler, F., Rezzolla, L., Stergioulas, N., Font, J.A., Seidel, E., (2005)

Collapse sequence for the slowly rotating model.

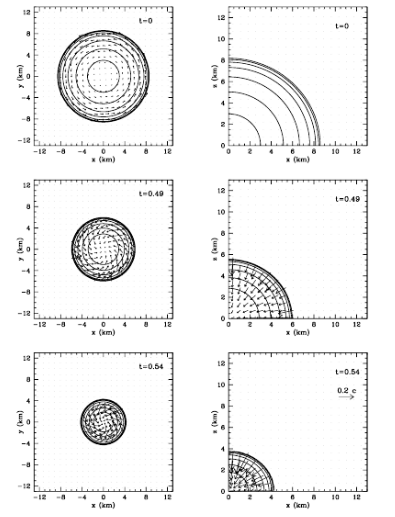

Collapse sequence for the rapidly rotating model.

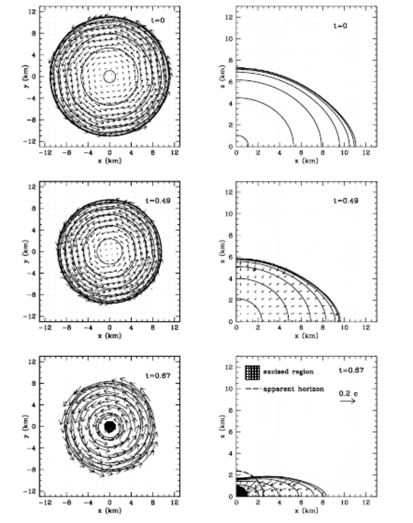

Astrophysical scenarios governed by relativistic (magneto-)hydrodynamical processes

Gamma-ray Bursts

- $v_{\mathrm{jet/wind}} \approx 0.99995c$
- $L_{\mathrm{GRB}} \approx 10^{52}$ erg/s ($T \approx 1 \ s$)
- Size: $\approx 1 \ pc$
- Collimation: few tens of degrees
- Central engine: stellar BH + torus

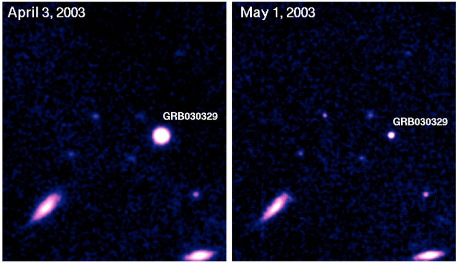

Image of Afterglow of GRB 030329
(VLT + FORS)

ESO PR Photo 17a/03 (18 June 2003)

©European Southern Observatory

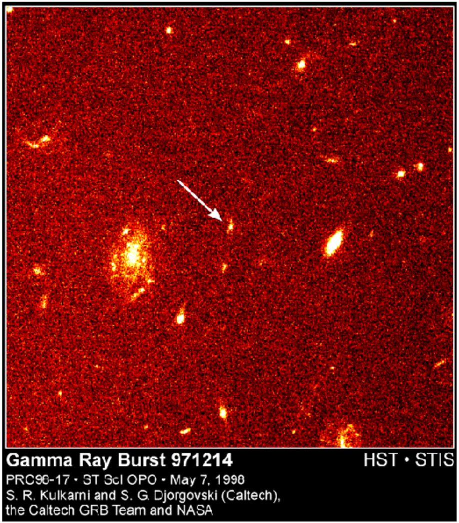

Gamma Ray Bursts: BATSE and Models of Progenitors

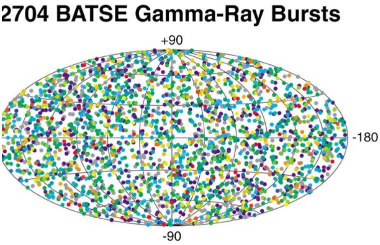

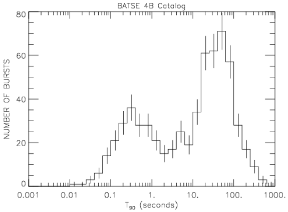

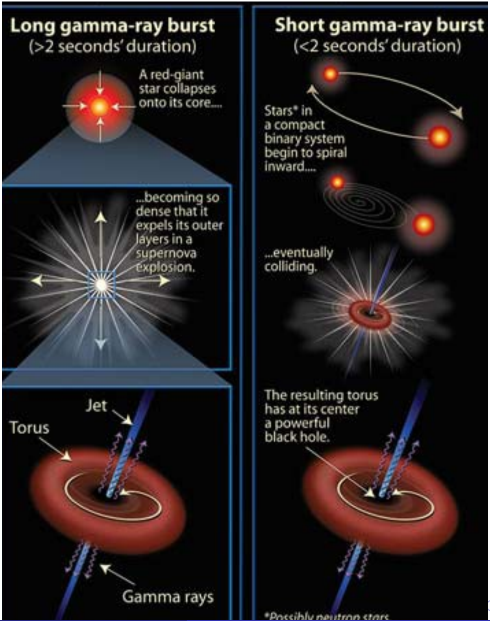

GRBs of long duration (lGRB): Relativistic Jets from Collapsars

Aloy, Müller, Ibáñez, Martí, MacFadyen (2000)

lGRBs: *Lorentz factor*

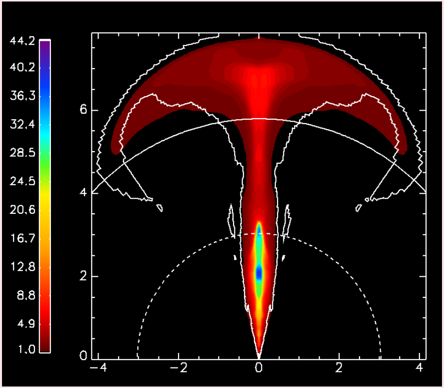

Lorentz factor about 1.8 s after shock breakout. The numbers on the axes give the length in units of 100,000 km. Dashed and solid arcs mark the stellar surface and the outer edge of the exponential stellar atmosphere, respectively. The other solid line encloses matter with a radial velocity larger than 0.3c, and an internal energy density larger than 5% of the rest-mass energy.

lGRBs: *Rest-mass density*

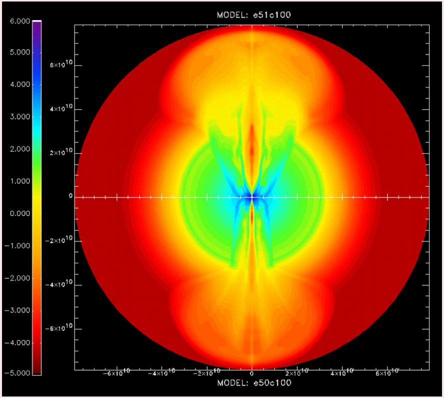

Rest-mass density for the models with a constant energy deposition rate of 10^{51} erg/s (top) and 10^{50} erg/s (bottom) respectively, about 1.8 s after shock breakout. The numbers on the axes give the length in units of centimeters.

Progenitors of sGRBs *Aloy, Janka, Müller (2005)*

Mergers of compact binaries: Relativistic Jets

- **Larger Lorentz Factors**
- **Larger opening angles (collimation due to the accretion torus)**
- **Less iso-energy.**
- **Prediction:**

The observed signature depends on the merger ambient density:
high density → UV-flash
low density → GRB

- **For the first time the viability of the merger of CB as progenitors of sGRBs is verified**

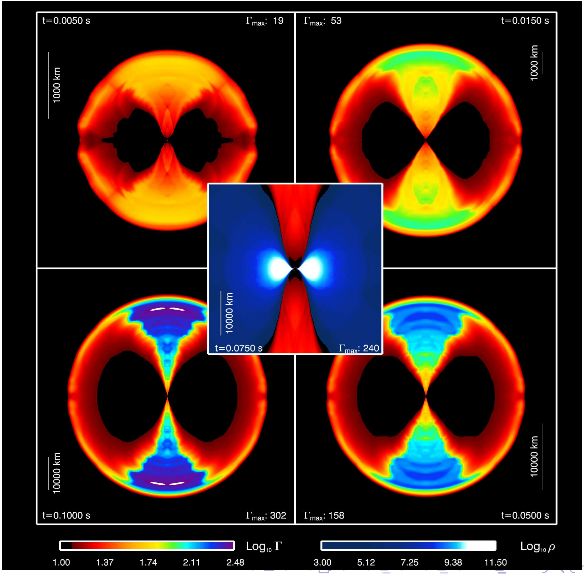

Bow shock Nebula Near Neutron Stars

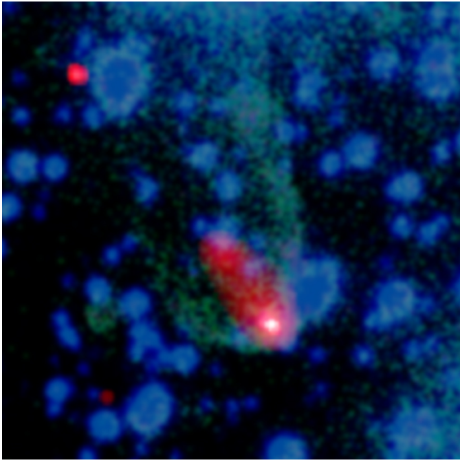

B1957+20 (Black Widow Pulsar)

A Cocoon Found Inside the Black Widow's Web **(Credit: X-ray: NASA/CXC/ASTRON/B.Stappers et al., Optical: AAO/J.Bland-Hawthorn & H.Jones)**

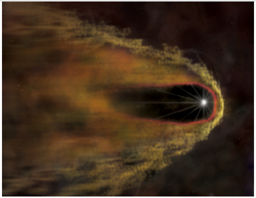

Artistic view of a bowshock nebula around a compact star

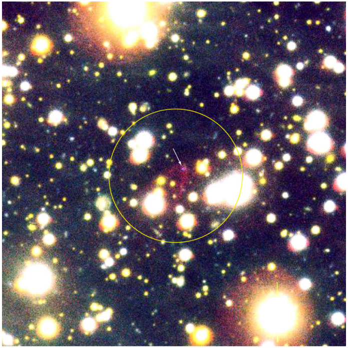

A Bowshock Nebula Near the Neutron Star RX J1856.5-3754 (Detail)
(VLT KUEYEN + FORS2)

Bondi-Hoyle Accretion onto a **Kerr Black Hole** *Font, Ibáñez & Papadopoulos, 1998*

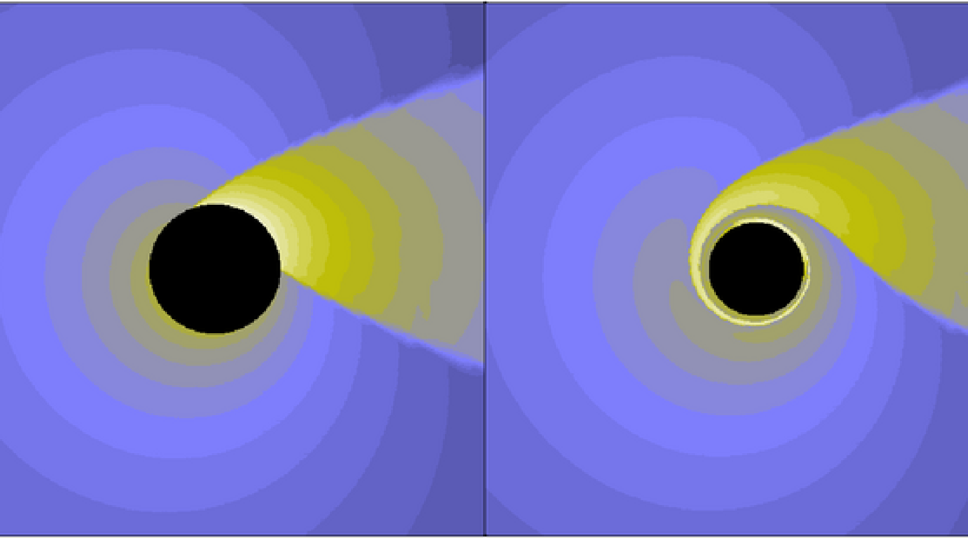

Magnetized accretion torus around a Kerr BH *McKinney & Gammie (2004)*

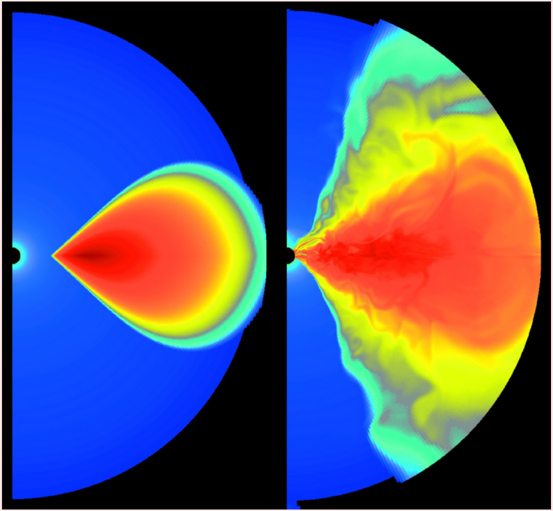

Initial *(left)* and final *(right)* distribution of $log\rho_0$ in the fiducial model on the $r\ sin\theta - r\ cos\theta$ plane. At $t = 0$, black corresponds to $\rho_0 \approx 4 \times 10^{-7}$ and dark red corresponds to $\rho_0 = 1$. Inner and outer radius are placed at $r = 6$ and $r = 42$, respectively (in units of the BH mass). At $t = 2000$, black corresponds to $\rho_0 \approx 4 \times 10^{-7}$ and dark red corresponds to $\rho_0 = 0.57$. The black half circle at the left edge is the black hole (Kerr BH with $a = 0.938$). *The initial state is perturbed by a weak poloidal magnetic field. It is*

Self-gravitating accretion tori around a BH *Montero, Font & Shibata (2010)*

Three snapshots: $t = 0, 2, 7$ (units of t_{orb})

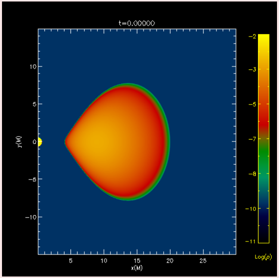

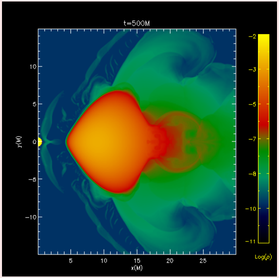

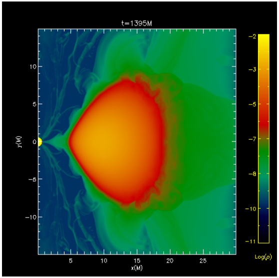

Captions

Figures show three different snapshots of the evolution of a self-gravitating torus, up to a final time of $t = 7\ t_{orb}$. The initial perturbation triggers the accretion of mass and angular momentum through the cusp and on to the BH . Our simulations show that such a quasi-periodic oscillatory behaviour, which had already been found in the test-fluid simulations of non-self-gravitating disks, is also present when the self-gravity and fully dynamical spacetime and hydrodynamical evolutions are incorporated in the numerical modelling. The colour coded iso density contours displayed also show the interesting dynamics at the boundary region separating the disk from the external medium. In particular, Kelvin-Helmhotz-driven eddies are seen being shed downwind from the edge of the disk during each oscillation
Parameters: $M_{torus}/M_{bh} = 1.0, r_{in} = 4.02, r_{out} = 19.97, t_{orbit} = 199.54$ (units of $G = c = M_{\odot} = M_{bh} = 1$)

Merger of binary neutron stars *Shibata, Taniguchi & Uryu (2005)*

Model SLy1313a $(NS + NS \rightarrow SMNS)$: $\Gamma_{\rm th} = 2$, $Grid = (633, 633, 317)$, $\lambda_0 = 316km$, $\lambda_{\rm merger} = 94km$

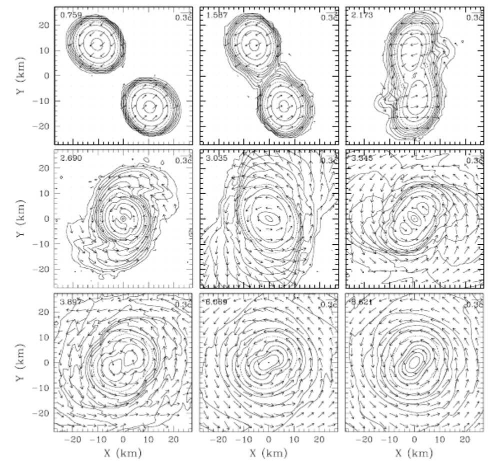

Snapshots of the **density contour** curves for ρ in the equatorial plane for model SLy1313a. The solid contour curves are drawn for $\rho = 2 \times 10^{14} \times i$ g/cm^3 $(i = 2 \sim 10)$ and for $2 \times 10^{14} \times 10^{-0.5i}$ g/cm^3 $(i = 1 \sim 7)$. The dotted curves denote 2×10^{14} g/cm^3. The initial orbital period in this case is 2.110 ms. Vectors indicate the local velocity field (v^x, v^y), and the scale is shown in the upper right-hand corner.

Merger of binary neutron stars *Shibata, Taniguchi & Uryu (2005)*

Model SLy1414a $(NS + NS \rightarrow BH)$: $\Gamma_{th} = 2$, $Grid = (633, 633, 317)$, $\lambda_0 = 302km$

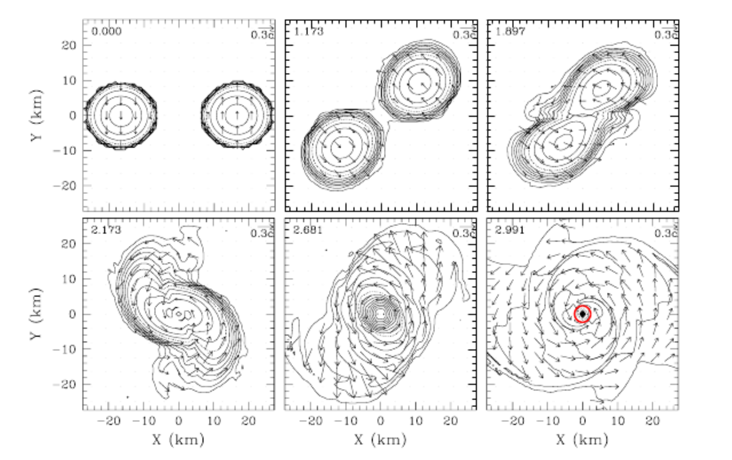

Snapshots of the **density contour** curves for ρ in the equatorial plane for model SLy1414a. The solid contour curves are drawn for $\rho = 2 \times 10^{14} \times i$ g/cm^3 $(i = 2 \sim 10)$ and for $2 \times 10^{14} \times 10^{-0.5i}$ g/cm^3 $(i = 1 \sim 7)$. The dotted curves denote 2×10^{14} g/cm^3. The initial orbital period in this case is 2.012 ms. The thick circle in the last panel of radius $r \sim 2$ km denotes the location of the apparent horizon.

Merger of binary neutron stars *Shibata, Taniguchi & Uryu (2005)*

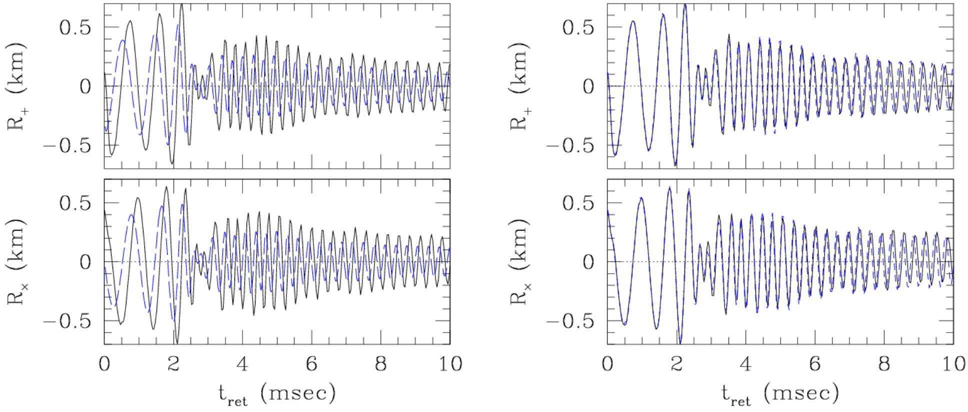

(Left) Gravitational waves for model SLy1313a. R_+ and $R_\times$ (solid curves) and A_+ and $A_\times$ (dashed curves) as functions of the retarded time are shown.
(Right) R_+ and $R_\times$ as functions of the retarded time for model SLy125135a (solid curves). For comparison, those for SLy1313a are shown by the dashed curves.

Coalescing neutron stars *Baiotti, Giacomazzo, Rezzolla (2010)*

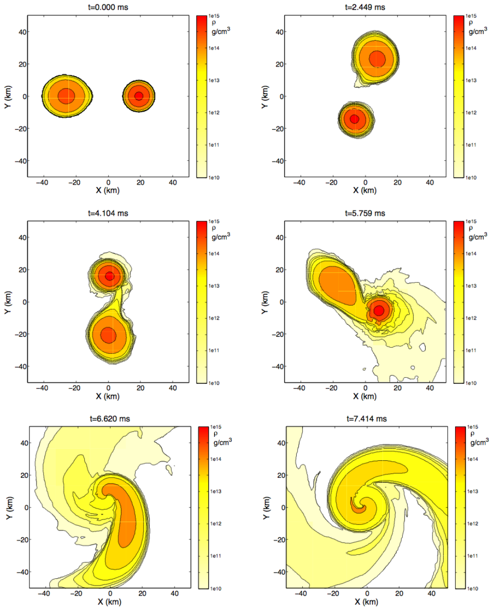

Coalescing neutron stars *Baiotti, Giacomazzo, Rezzolla (2010)*

Imprint of the EOS: Ideal fluid vs polytropic

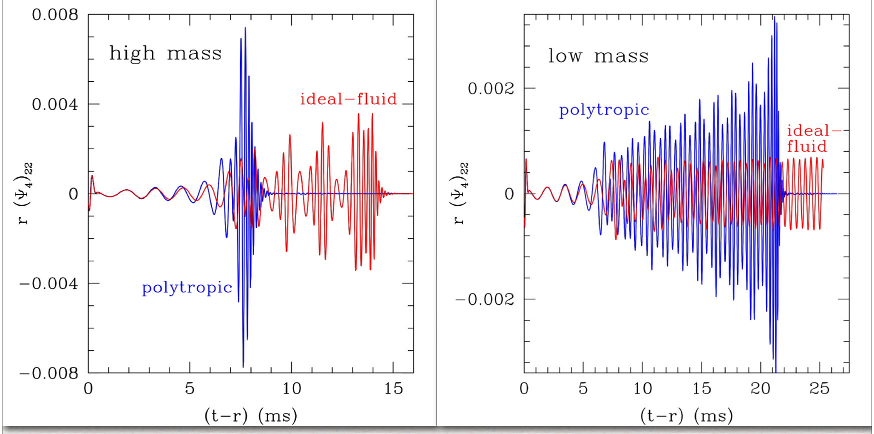

After the merger a BH is produced over a timescale comparable with the dynamical one

After the merger a BH is produced over a timescale larger or much larger than the dynamical one

Magnetized Kelvin-Helmholtz instability in NS-mergers *Obergaulinger, Aloy, Müller (2010)*

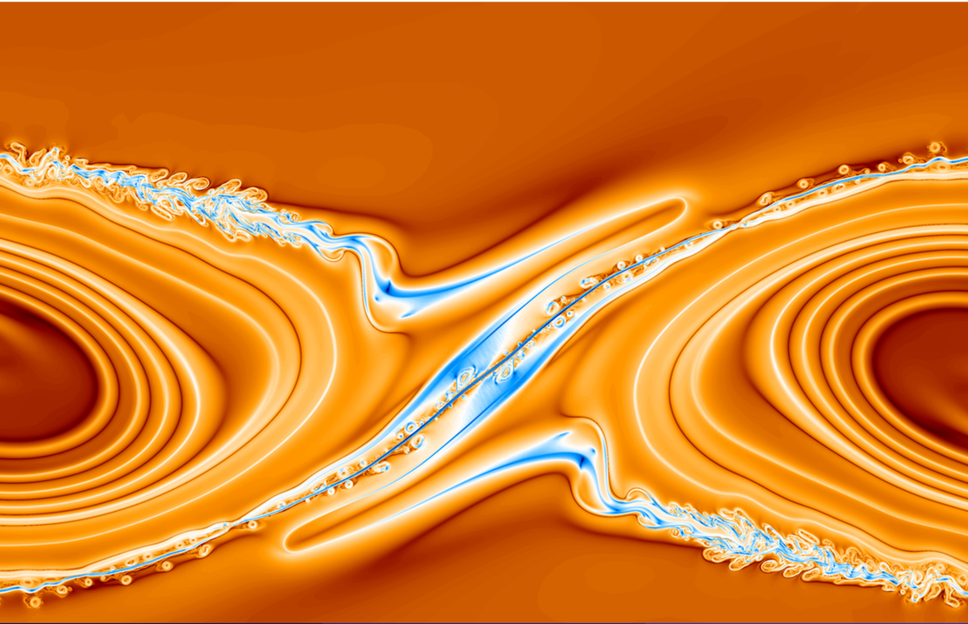

Astrophysical scenarios governed by relativistic (magneto-)hydrodynamical processes

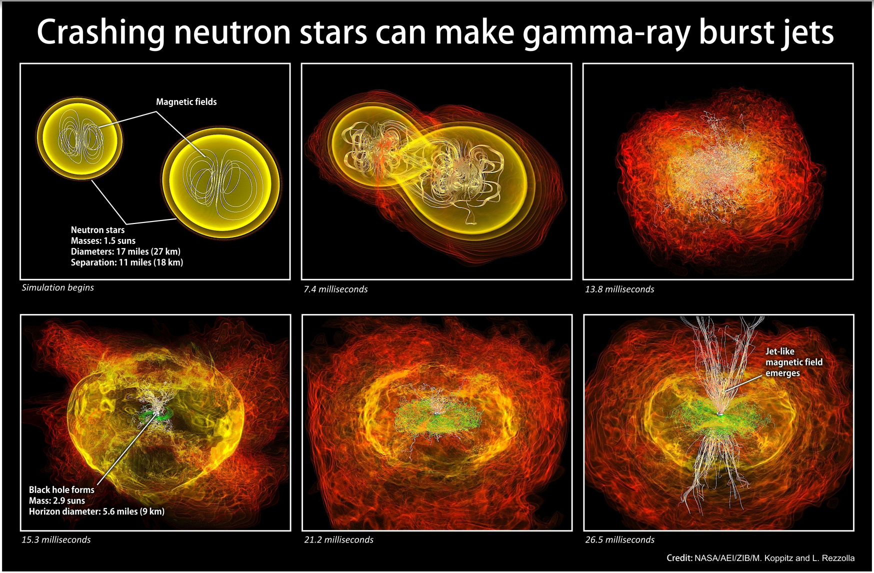

Merging neutron stars produce jet-like structures and can power short Gamma-Ray Bursts

(Rezzolla, Giacomazzo, Baiotti, Granot, Kouveliotou, Aloy, 2011)

Outline

Two Micron All Sky Survey (2MASS): $\approx 1.5\,10^6$ *stars and galaxies in the nearby universe*

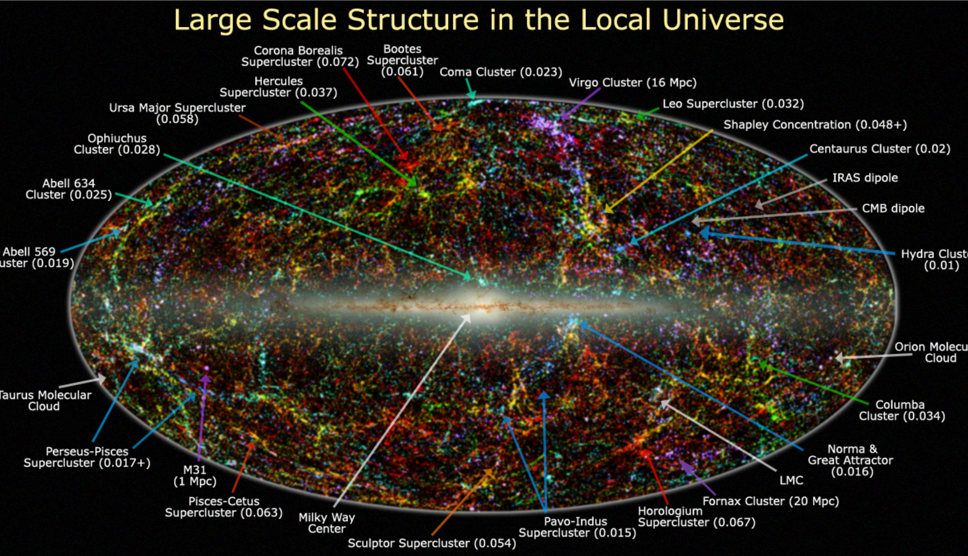

Legend: image shows 2MASS galaxies color coded by redshift (Jarrett 2004); familiar galaxy clusters/superclusters are labeled (numbers in parenthesis represent redshift). Graphic created by T. Jarrett (IPAC/Caltech)

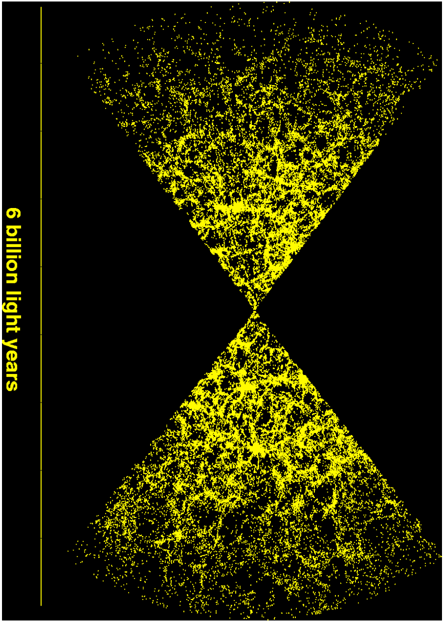
6 billion light years

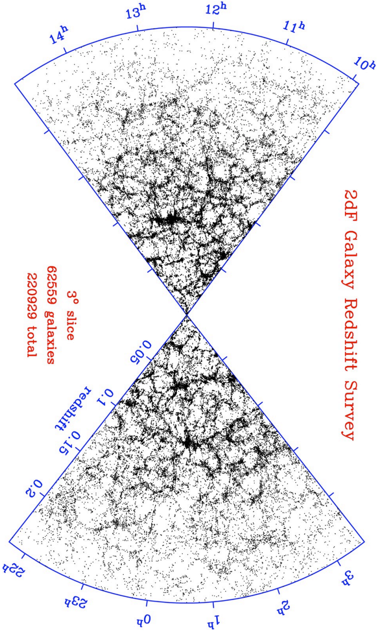
2dF Galaxy Redshift Survey
3° slice
62559 galaxies
220929 total
redshift
0.05
0.1
0.15
0.2
14h
13h
12h
11h
10h
22h
23h
0h
1h
2h
3h

Departament d'Astronomia i Astrofísica
VNIVERSITAT DE VALÈNCIA

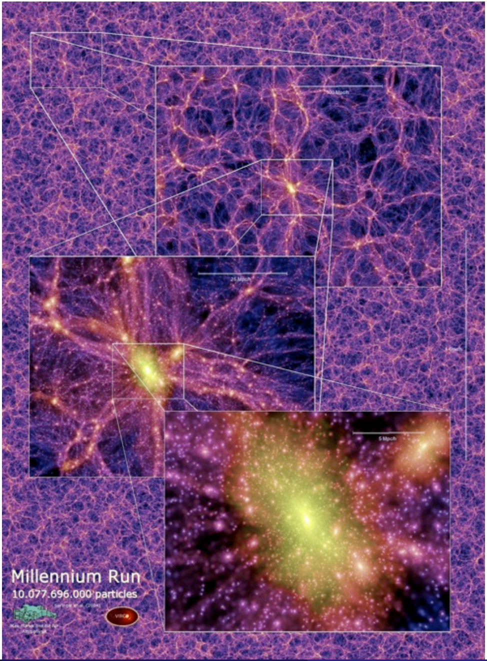

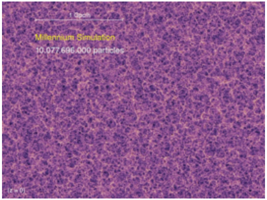

10^{10} particles
512 CPUs
343000 hours
Volume: 9 Gpc^3

Computational Cosmology: HSCL *Peebles (1980); Quilis, Ibáñez & Sáez (1994)*

$$\frac{\partial \vec{u}}{\partial t} + \frac{\partial \vec{f}(\vec{u})}{\partial x} + \frac{\partial \vec{g}(\vec{u})}{\partial y} + \frac{\partial \vec{h}(\vec{u})}{\partial z} = \vec{s}(\vec{u})$$

$\vec{u} : \Re \times \Re^3 \rightarrow \Re^5$ is the vector of *unknowns*:

$$\vec{u} = [\delta, m_x, m_y, m_z, E] \quad ,$$

$\vec{F}^\alpha \equiv \{\vec{f}, \vec{g}, \vec{h}\}$ are the three *flux* functions in the spatial directions x, y, z: $\Re^5 \rightarrow \Re^5$:

$$\vec{f}(\vec{u}) = \left[\frac{m_x}{a}, \frac{m_x^2}{(\delta+1)a} + \frac{p}{a\rho_B}, \frac{m_x m_y}{(\delta+1)a}, \frac{m_x m_z}{(\delta+1)a}, \frac{(E+p)m_x}{a(\delta+1)}\right]$$

$$\vec{g}(\vec{u}) = \left[\frac{m_y}{a}, \frac{m_x m_y}{(\delta+1)a}, \frac{m_y^2}{(\delta+1)a} + \frac{p}{a\rho_B}, \frac{m_y m_z}{(\delta+1)a}, \frac{(E+p)m_y}{a(\delta+1)}\right]$$

$$\vec{h}(\vec{u}) = \left[\frac{m_z}{a}, \frac{m_x m_z}{(\delta+1)a}, \frac{m_y m_z}{(\delta+1)a}, \frac{m_z^2}{(\delta+1)a} + \frac{p}{a\rho_B}, \frac{(E+p)m_z}{a(\delta+1)}\right]$$

Computational Cosmology: HSCL *Peebles (1980); Quilis, Ibáñez & Sáez (1994)*

$$\frac{\partial \vec{u}}{\partial t} + \frac{\partial \vec{f}(\vec{u})}{\partial x} + \frac{\partial \vec{g}(\vec{u})}{\partial y} + \frac{\partial \vec{h}(\vec{u})}{\partial z} = \vec{s}(\vec{u})$$

$\vec{s} : \Re^5 \rightarrow \Re^5$ are the *sources*:

$$\vec{s}(\vec{u}) = [0 \quad , - \quad \frac{(\delta+1)}{a}\frac{\partial \phi}{\partial x} - Hm_x, -\frac{(\delta+1)}{a}\frac{\partial \phi}{\partial y} - Hm_y, -\frac{(\delta+1)}{a}\frac{\partial \phi}{\partial z} - Hm_z,$$
$$- \quad 3H(E+p) - \frac{\rho_B H m^2}{(\delta+1)} - \frac{m_x \rho_B}{a}\frac{\partial \phi}{\partial x} - \frac{m_y \rho_B}{a}\frac{\partial \phi}{\partial y} - \frac{m_z \rho_B}{a}\frac{\partial \phi}{\partial z}]$$

- $\vec{x}$: the Eulerian coordinates.
- $\vec{v} = a(t)\frac{d\vec{x}}{dt} = (v_x, v_y, v_z)$: the peculiar velocity.
- $m_i := (\delta+1)v_i$ (i=x,y,z)
- $E = \rho\epsilon + \frac{1}{2}\rho v^2$ $(v^2 = v_x^2 + v_y^2 + v_z^2)$: the total energy.
- $\phi(t, \vec{x})$ is the peculiar Newtonian gravitational potential: $\nabla^2\phi = \frac{3}{2}H^2 a^2 \delta$
- An *equation of state* $p = p(\rho, \epsilon)$ closes the system.

Eigenvalues: $\lambda^x_\pm = \frac{v_x \pm c_s}{a} \quad , \quad \lambda^x_\pm = \frac{v_x}{a} \quad (triple)$

Computational Cosmology: Stellar Dawn (Pop III) *M. Norman et al. (2003)*

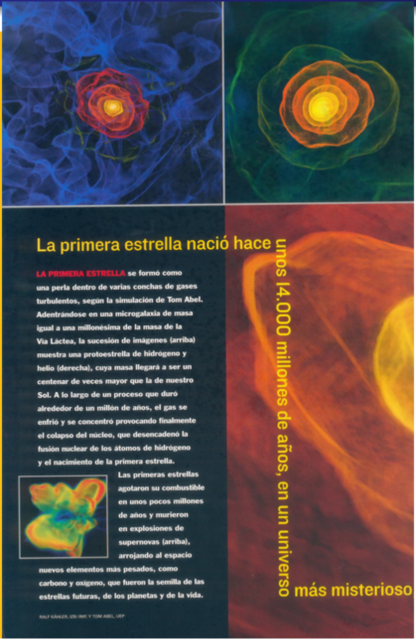

La primera estrella nació hace unos 14.000 millones de años, en un universo más misterioso

LA PRIMERA ESTRELLA se formó como una perla dentro de varias conchas de gases turbulentos, según la simulación de Tom Abel. Adentrándose en una microgalaxia de masa igual a una millonésima de la masa de la Vía Láctea, la sucesión de imágenes (arriba) muestra una protoestrella de hidrógeno y helio (derecha), cuya masa llegará a ser un centenar de veces mayor que la de nuestro Sol. A lo largo de un proceso que duró alrededor de un millón de años, el gas se enfrió y se concentró provocando finalmente el colapso del núcleo, que desencadenó la fusión nuclear de los átomos de hidrógeno y el nacimiento de la primera estrella.

Las primeras estrellas agotaron su combustible en unos pocos millones de años y murieron en explosiones de supernovas (arriba), arrojando al espacio nuevos elementos más pesados, como carbono y oxígeno, que fueron la semilla de las estrellas futuras, de los planetas y de la vida.

Computational Cosmology: Stellar Dawn (Pop III) *M. Norman et al. (2003)*

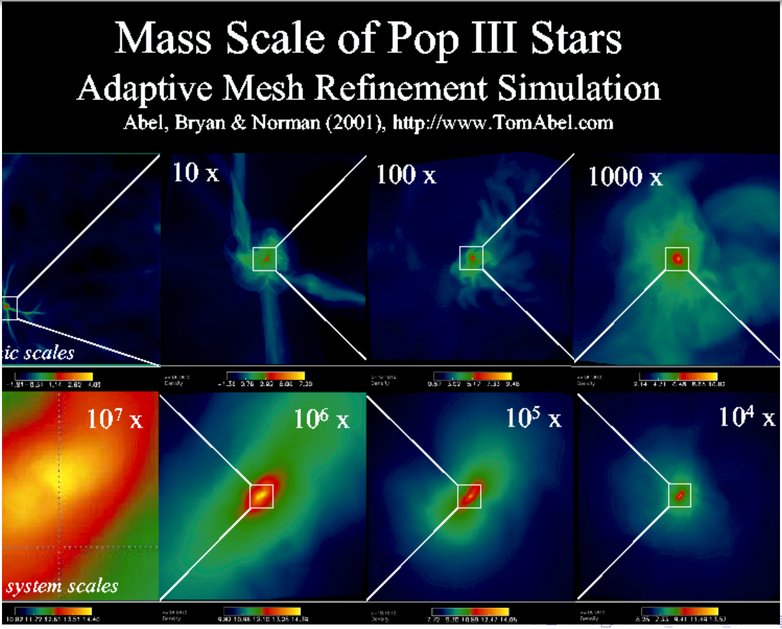

Mergers of Galaxy Clusters with MASCLET @ $z = 0.12$ it Planelles & Quilis (2009)

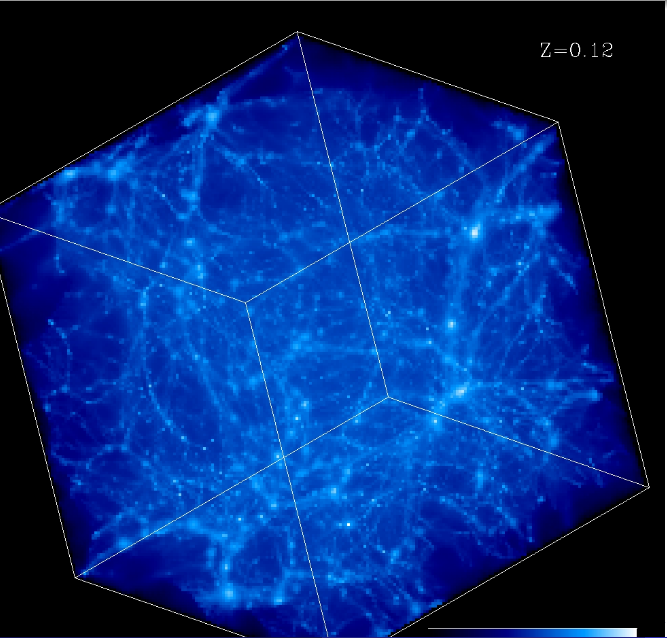

The role of the mergers of clusters as a source of feedback has been explored. The simulations have shown that mergers can explain the two broad populations in which galaxy clusters split. *Gas, DM, Compton and Bremsstrahlung cooling, star formation, and SNe feedback.*

Cosmological shock waves: clues to the formation history of haloes *Planelles & Quilis (2012)*

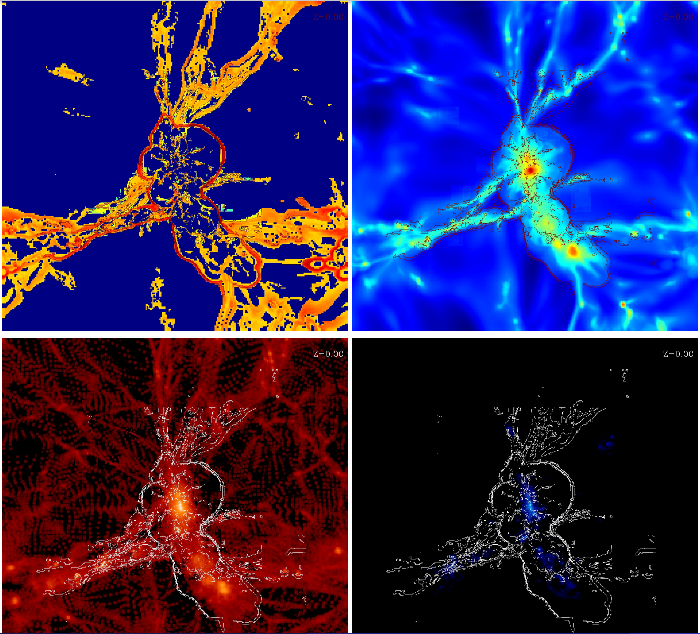

Distributions of Mach number compared with dark matter, gas and stellar densities at $z = 0$. Each panel is a slice of 0.2 Mpc thickness and 64 Mpc side length. They show the Mach number distribution (upper left) and the gas, dark matter and stellar densities (upper right, lower left, and lower right panels, respectively). All these quantities are in logarithmic scale. In all the panels, we overplot ***the contours of the shock waves*** *developed during the formation and evolution of cosmic structures.*

Formation of galaxies in ΛCDM cosmologies: The fine structure of disc galaxies

Doménech-Moral, Martínez-Serrano, Domínguez-Tenreiro & Serna (2012)

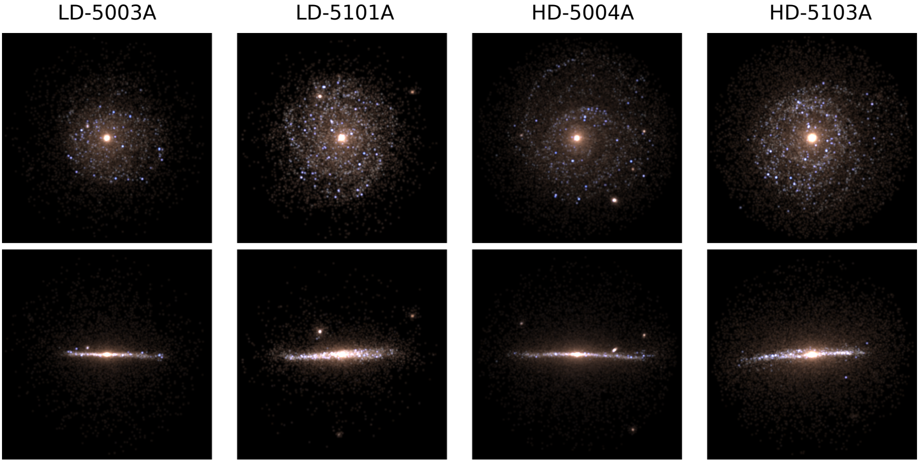

Face-on and edge-on synthetic images of the four main simulated objects at $z = 0$. *In all these images, a conspicuous disc component can be appreciated even for the object HD-5103A, where the disc structure has survived a recent major merger at* $z \sim 0.3$. *All images are 40 kpc side.* **DEVA**

The 'Valencian-GALAXY-zoo'

Javier Navarro-González, Elena Ricciardelli, Vicent Quilis, Alexandre Vazdekis

$> \nu/\sigma >$

$> \epsilon >$

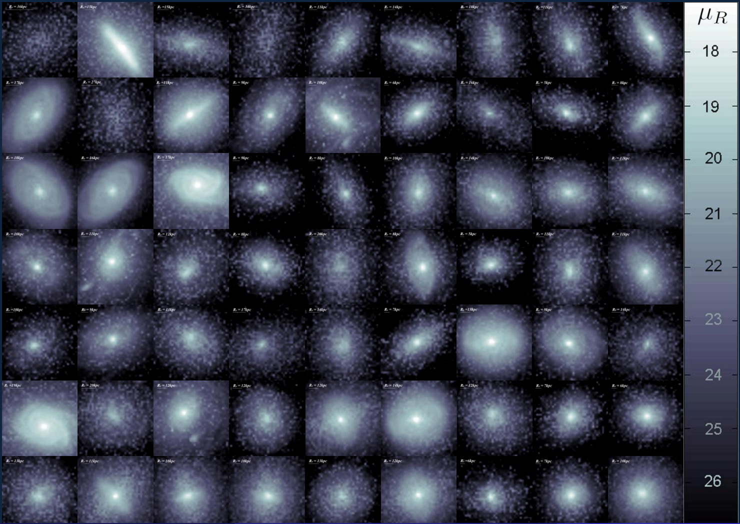

+

Gone with the wind: the origin of SO galaxies in clusters *Quilis, Moore, Bower (2000)*

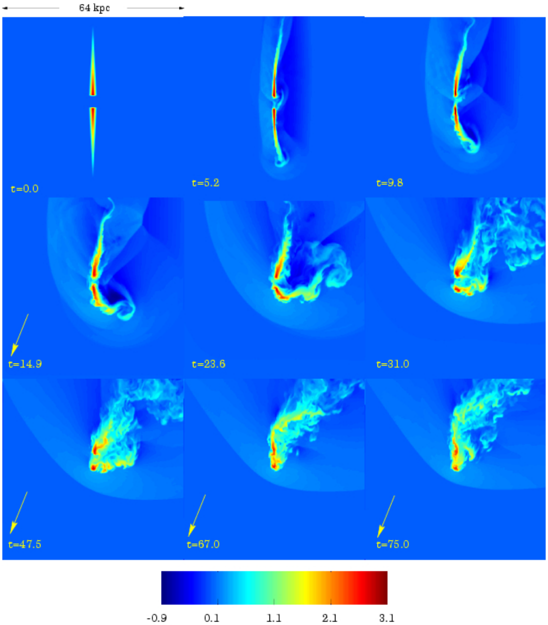

Galactic Metamorphosis

The evolution of the gaseous disk of a spiral galaxy moving face-on to the direction of motion through a diffuse hot intracluster medium (ICM). Each snapshot shows the density of gas $(\delta = \frac{\rho}{\rho_{ICM}})$ within a 0.2-kpc slice through the center of the galaxy and each frame is 64 kpc on a side. Note how rapidly the disk material is removed: within 100 My, 100% of the HI is lost. The box size is $64\ kpc$ and the hydro grid has 256^3 cells.

Intracluster Medium reheating by relativistic jets *Perucho, Quilis & Martí (2012)*

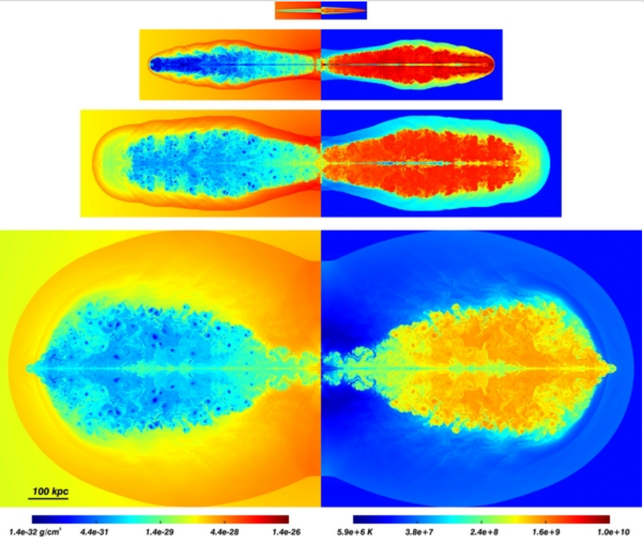

Four snapshots. After the jet switch-off, the channel opened by the jet is still seen on the axis in the third and fourth frames although the jet terminal shock has already disappeared.

GHALO: A Galactic mass DM halo

Stadel, Potter, Moore, Diemand, Madau, Zemp, Kuhlen & Quilis (2010)

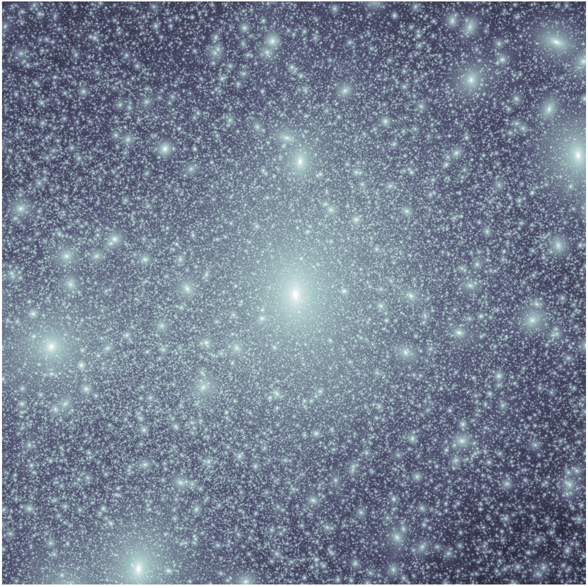

The density of dark matter within the inner 200 kpc of GHALO$_2$. There are about 100,000 subhaloes that orbit within the virial radius. Each bright spot in this image is an individual, bound, dark matter subhalo made up of many thousands of particles (there are far more particles than pixels here). Over three billion particles and a mass resolution of $1000 M_{\odot}$.

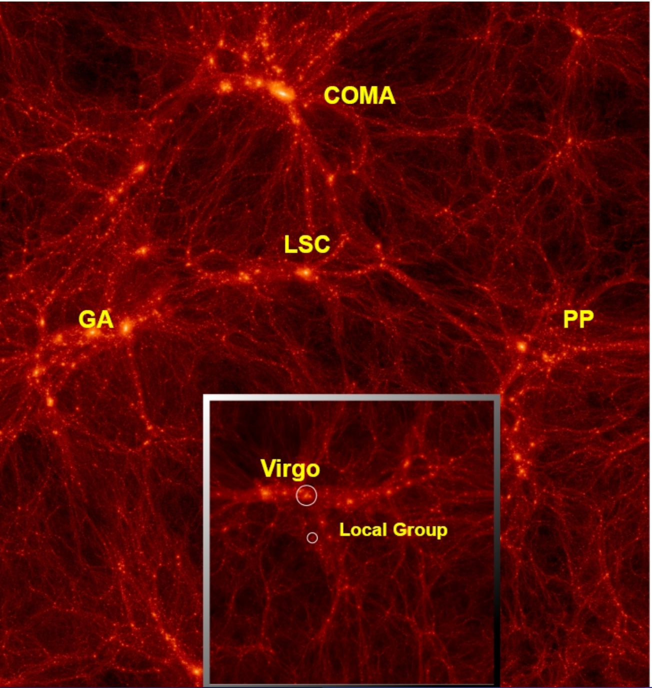

CLUES:
DM @ the Local Universe

Large scale Dark Matter density distribution of the Local Universe. A combination of two slices from two different CLUES simulations within a WMAP 3 cosmology. The Local Supercluster (LSC) forms in both simulations and matches pretty well, despite the fact that the realizations were different.

GA = Great Attractor
PP = Perseus-Pisces-Cluster
CLUES ≡ Constrained Local UniversE Simulations

Stefan Gottlöber, Yehuda Hoffman, Anatoly Klypin & Gustavo Yepes

www.clues-project.org

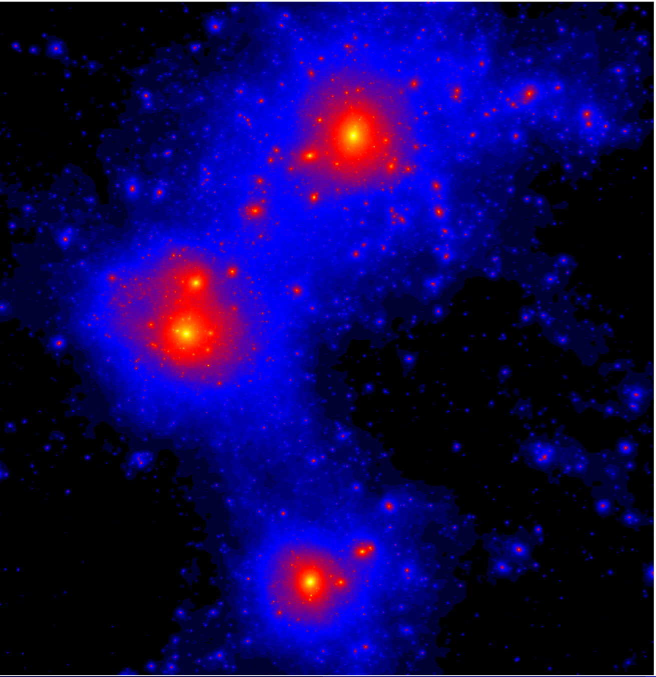

CLUES:
Dark Matter distribution of the Local Group

Projection along the z-direction of the three main halos: MW (up), M31 (center) and M33 (bottom). The shown box has a size of 1.3 Mpc/h per side.
CLUES ≡ Constrained Local UniversE Simulations
Stefan Gottlöber, Yehuda Hoffman, Anatoly Klypin & Gustavo Yepes
www.clues-project.org

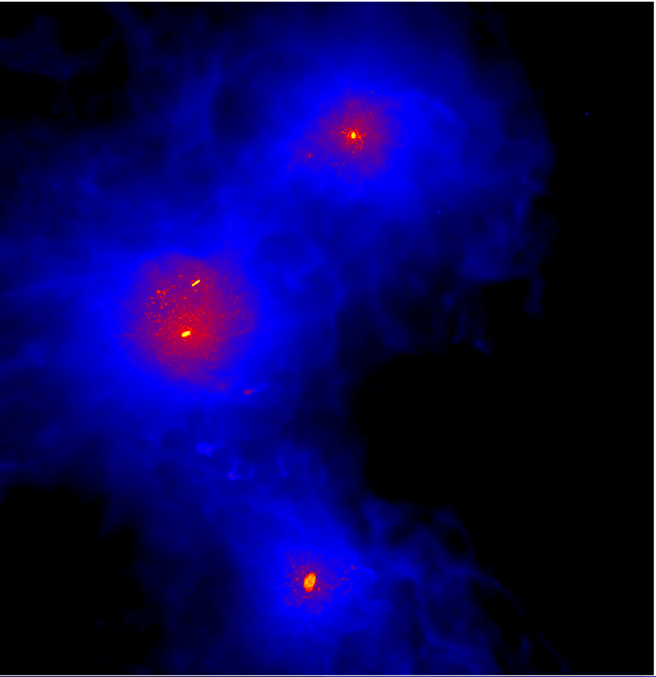

CLUES: *Gas distribution of the Local Group*

Projection along the z-direction of the three main halos: MW (up), M31 (center) and M33 (bottom). The shown box has a size of 1.3 Mpc/h per side.
CLUES ≡ Constrained Local UniversE Simulations
Stefan Gottlöber, Yehuda Hoffman, Anatoly Klypin & Gustavo Yepes
www.clues-project.org

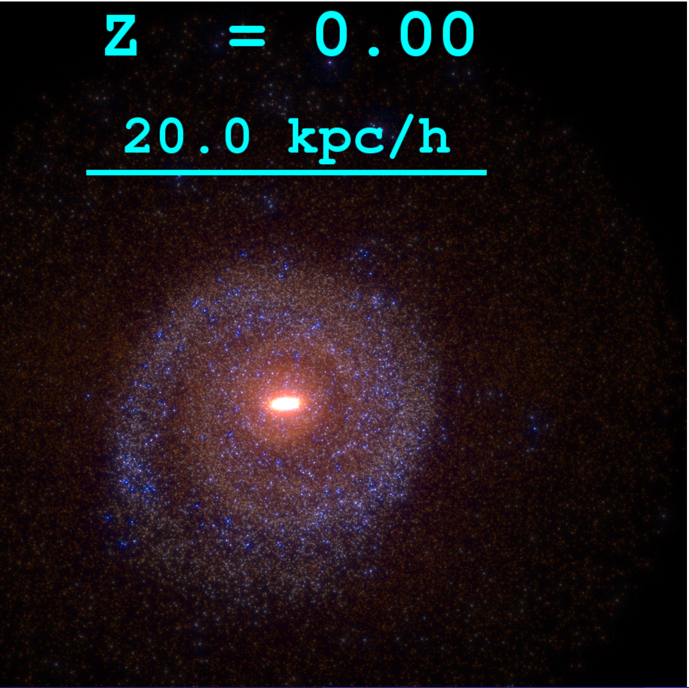

CLUES:
The Milky Way

Stellar disk of the Milky Way in the Constrained Simulation of the Local Group (WMAP3), as it might be seen from a Hubble Space Telescope at a different galaxy. Face-on. Blue dots mark extremely hot and massive stars, red dots resemble old and cold stellar populations.
CLUES ≡ Constrained Local UniversE Simulations
Stefan Gottlöber, Yehuda Hoffman, Anatoly Klypin & Gustavo Yepes
www.clues-project.org

Outline

Some Numerical Codes (public domain)

- **CLAWPACK** → **http://www.amath.washington.edu/ claw/**
  CLAWPACK is a software package developed at the Department of Applied Mathematics of the University of Washington, to compute numerical solutions to hyperbolic partial differential equations using a wave propagation approach.
- **ZEUS 3D** → **http://lca.ucsd.edu/portal/software/zeus-3d**
  ZEUS-3D is a computational fluid dynamics code developed at the Laboratory for Computational Astrophysics (NCSA, University of Illinois at Urbana-Champaign) for the simulation of astrophysical phenomena.
- **FLASH** → **http://flash.uchicago.edu/website/home/**
  FLASH is developed at the ASC/Alliances Center for Astrophysical Thermonuclear Flashes to solve the long-standing problem of thermonuclear flashes on the surfaces of compact stars such as neutron stars and white dwarf stars, and in the interior of white dwarfs (i.e., Type Ia supernovae). The Center is based at the University of Chicago, and involves collaboration between faculty and staff from several University of Chicago departments and institutes, the Mathematics and Computer Science division of Argonne National Laboratory, and the Rensselaer Polytechnic Institute. ASC / Alliances Center for Astrophysical Thermonuclear Flashes is one of five Advanced Simulation and Computing (ASC) Academic Strategic Alliances Program (ASAP) centers.

Some Numerical Codes (public domain)

- **GADGET → http://www.mpa-garching.mpg.de/gadget/**
  GADGET is a freely available code for cosmological N-body/SPH simulations on massively parallel computers with distributed memory. GADGET uses an explicit communication model that is implemented with the standardized MPI communication interface. GADGET has been developed by V. Springel at the Max-Planck Institut für Astrophysik (Garching, Germany).
- **CACTUS → http://www.cactuscode.org/**
  CACTUS is an open source problem solving environment designed for scientists and engineers. Its modular structure easily enables parallel computation across different architectures and collaborative code development between different groups. CACTUS originated in the academic research community, where it was developed and used over many years by a large international collaboration of physicists and computational scientists.
- **WHISKY, CoCoNuT (private)**
  GRHD-codes to evolve the equations of hydrodynamics on curved space-time. WHISKY was written by and for members of the EU Network on Sources of Gravitational Radiation and is based on the Cactus Computational Toolkit . CoCoNuT has been written by and for members of the Garching-Meudon-Valencia groups (and collaborators). These two codes differ in the strategy (theoretical and numerical) to solve Einstein Equations.

Summary: Benefits

- Supercomputing allows one *to replace or complement the experimentation/observation*, generally much more expensive.
- Supercomputing allows one *to keep control on the experiments* in a more precise way than in laboratory. It avoids to carry out experiments potentially dangerous for the human beings or their environment (e.g., nuclear weapons testing).
- Supercomputing allows one *to check physical/mathematical models* that otherwise could not been possible to verify (e.g., astrophysical models).
- Supercomputing allows one *to develop new theories* and more sophisticated analytical models.
- Supercomputing has become *an essential tool for scientific and technological progress in the areas of science and engineering*. It's been told that supercomputers will play for the Science of XXI century, the same role that Mathematics played for the Physics progress during last two centuries.

ASTRONET: A Science Vision for European Astronomy

Recommendations (Cross disciplinary requirements)

Theory and Simulations

Astronomy has evolved from a following science (applying fundamental results from other fields), to a leading science (astronomical discoveries and interpretations inspire other fields). In order to maintain this position, and to remain able to interpret and guide future observations, *continued investments have to be made into the development of theory and simulations*.

ASTRONET: A Science Vision for European Astronomy

Recommendations (Cross disciplinary requirements)

Theory and Simulations

Astronomy has evolved from a following science (applying fundamental results from other fields), to a leading science (astronomical discoveries and interpretations inspire other fields). In order to maintain this position, and to remain able to interpret and guide future observations, *continued investments have to be made into the development of theory and simulations*.

Computing resources

Substantial high-performance computing resources will be mandatory, not only for processing and analysis of the extensive observational data, but also for the theoretical calculations and simulations including detailed physical processes and feedback mechanisms. The combination of these two aspects is crucial for careful comparison of observational datasets and theoretical predictions.

Final Remarks

Final Remarks

Message: SA

Final Remarks

Message: SA

S upercomputing $\Longrightarrow$ A dvance in theory/prediction/explanation

Final Remarks

Message: SA

S upercomputing $\Longrightarrow$ A dvance in theory/prediction/explanation

Message: SO

Final Remarks

Message: SA

S upercomputing $\Longrightarrow$ A dvance in theory/prediction/explanation

Message: SO

S upercomputing (Supercomputers) $\approx$ O bservations (Telescopes)

Final Remarks

Message: SA

S upercomputing $\Longrightarrow$ A dvance in theory/prediction/explanation

Message: SO

S upercomputing (Supercomputers) $\approx$ O bservations (Telescopes)

Message: FF

Final Remarks

Message: SA

S upercomputing $\Longrightarrow$ A dvance in theory/prediction/explanation

Message: SO

S upercomputing (Supercomputers) $\approx$ O bservations (Telescopes)

Message: FF

F ailures (in Computing) F oster (for new algorithms)

Final Remarks

Message: SA

S upercomputing $\Longrightarrow$ A dvance in theory/prediction/explanation

Message: SO

S upercomputing (Supercomputers) $\approx$ O bservations (Telescopes)

Message: FF

F ailures (in Computing) F oster (for new algorithms)

Message: EE

Final Remarks

Message: SA

S upercomputing $\Longrightarrow$ A dvance in theory/prediction/explanation

Message: SO

S upercomputing (Supercomputers) $\approx$ O bservations (Telescopes)

Message: FF

F ailures (in Computing) F oster (for new algorithms)

Message: EE

New programming paradigms for the near future E xascale E ra